Monthly Notices
of the
ROYAL ASTRONOMICAL SOCIETY

Mon. Not. R. Astron. Soc. **399,** 2249–2263 (2009) doi:10.1111/j.1365-2966.2009.15427.x

Mass and spin co-evolution during the alignment of a black hole in a warped accretion disc

A. Perego,[1⋆] M. Dotti,[2] M. Colpi[3] and M. Volonteri[2]

[1]*Department of Physics, University of Basel, Klingelbergstr. 82, 4056 Basel, Switzerland*
[2]*Department of Astronomy, University of Michigan, Ann Arbor, MI 48109, USA*
[3]*Dipartimento di Fisica, Università degli Studi di Milano-Bicocca, Piazza Della Scienza 3, 20126 Milano, Italy*

Accepted 2009 July 20. Received 2009 July 20; in original form 2009 March 16

ABSTRACT

In this paper, we explore the gravitomagnetic interaction of a black hole (BH) with a misaligned accretion disc to study BH spin *precession* and *alignment* jointly with BH mass $M_{\rm BH}$ and spin parameter a evolution, under the assumption that the disc is continually fed, in its outer region, by matter with angular momentum fixed on a given direction $\hat{\boldsymbol{J}}_{\rm disc,out}$. We develop an iterative scheme based on the adiabatic approximation to study the BH–disc co-evolution: in this approach, the accretion disc transits through a sequence of quasi-steady warped states (Bardeen–Petterson effect) and interacts with the BH until the spin $\boldsymbol{J}_{\rm BH}$ aligns with $\hat{\boldsymbol{J}}_{\rm disc,out}$. For a BH aligning with a corotating disc, the fractional increase in mass is typically less than a few per cent, while the spin modulus can increase up to a few tens of per cent. The alignment time-scale $t_{\rm al} \propto a^{5/7}\dot{M}^{-32/35}$ is of $\sim 10^5$–10^6 yr for a maximally rotating BH accreting at the Eddington rate. BH–disc alignment from an initially counter-rotating disc tends to be more efficient compared to the specular corotating case due to the asymmetry seeded in the Kerr metric: counter-rotating matter carries a larger and opposite angular momentum when crossing the innermost stable orbit, so that the spin modulus decreases faster and so the relative inclination angle.

Key words: accretion, accretion discs – black hole physics – galaxies: active – galaxies: evolution – quasars: general.

1 INTRODUCTION

Astrophysical black holes (BHs) are Kerr BHs fully characterized by their mass $M_{\rm BH}$ and spin $\boldsymbol{J}_{\rm BH}$, customarily expressed in terms of the dimensionless spin parameter a (≤ 1), and unit vector $\hat{\boldsymbol{J}}_{\rm BH}$:

$$\boldsymbol{J}_{\rm BH} = a\frac{GM_{\rm BH}^2}{c}\hat{\boldsymbol{J}}_{\rm BH}. \quad (1)$$

The spin and mass of BHs residing in galaxy nuclei do not remain constant, close to their birth values, but change sizeably through cosmic time, in response to major accretion events. In current cosmological scenarios for the evolution of galaxies, repeated interactions among gas-rich haloes play a key role not only in shaping galaxies, but also in triggering quasar activity (White & Rees 1978; Di Matteo, Springel & Hernquist 2005). Massive gaseous nuclear discs that form in the aftermath of major galaxy mergers (Mihos & Hernquist 1996; Mayer et al. 2007) may provide enough fuel to feed, on sub-parsec scales, the BH through a Keplerian accretion disc (Dotti et al. 2007, 2009). If these episodes repeat recursively and/or at random phases (King & Pringle 2006), the BH spin $\boldsymbol{J}_{\rm BH}$ is expected, initially, to be misaligned relative to the direction of the angular momentum of the disc $\hat{\boldsymbol{J}}_{\rm disc,out}$ at its unperturbed, outer edge $R_{\rm out}$. In this configuration, the gas elements inside the disc undergo Lense–Thirring precession (see e.g. Wilkins 1972). In the fluid, the action of viscosity on to the differentially precessing disc ensures that the inner portion of the accretion disc aligns (or anti-aligns) its orbital angular momentum with the BH spin $\boldsymbol{J}_{\rm BH}$, out to a transition radius $R_{\rm warp}$ beyond which the disc remains aligned to the outer disc, as first shown by Bardeen & Petterson (1975) (see also Armitage & Natarajan 1999; Nelson & Papaloizou 2000; Fragile & Anninos 2005; Fragile et al. 2007). Warping of the inner disc at distance R from the BH is communicated through the fluid elements on a time-scale $t_{\rm BP}(R)$ related to the vertical shear viscosity of the accretion disc. Therefore, the inner regions of the disc align (or counteralign if the disc is counter rotating) with the BH spin on the scale $t_{\rm BP}(R_{\rm warp})$ when the viscous time for vertical propagation of disturbances equals the Lense–Thirring precession time. On a longer time-scale, the joint evolution of BH+disc system restores full axisymmetry, with the BH spin direction aligned relative to the total angular momentum of the composite system (Rees 1978; Thorne, Price & MacDonald 1986; King et al. 2005). The change in

⋆E-mail: albino.perego@unibas.ch

$\boldsymbol{J}_{\rm BH}$ is a consequence of angular momentum conservation: since the BH acts on the disc with a torque that warps the disc then an equal and opposite gravitomagnetic torque acts on the BH that modifies its direction *only*.

BH spin alignment has been studied in two main contexts. In the first, explored by King et al. (2005) and Lodato & Pringle (2006), the focus is on an *closed* system where the accretion disc has a finite mass and radial extent. Here, the total angular momentum $\boldsymbol{J}_{\rm tot} = \boldsymbol{J}_{\rm BH} + \boldsymbol{J}_{\rm disc}$ is well-defined vector, and the BH eventually aligns it spin vector to the direction of $\boldsymbol{J}_{\rm tot}$. In the second, explored by Scheuer & Feiler (1996), Natarajan & Armitage (1999) and Martin, Pringle & Tout (2007), the focus is on an *open* system, where the accretion disc has infinite extension and it is continually fed at its outer edge by matter whose angular momentum has constant direction $\hat{\boldsymbol{J}}_{\rm disc,out}$. In this second case, the BH aligns its spin to the outer disc direction $\hat{\boldsymbol{J}}_{\rm disc,out}$ on a time-scale $t_{\rm al}$ that exceeds $t_{\rm BP}$ by a few orders of magnitude (Scheuer & Feiler 1996; Martin et al. 2007).

In this paper, we progress on the study of BH alignment including the contemporary change in mass and spin modulus due to accretion of matter, neglected in previous works. During BH precession and alignment, matter flows inwards and accretes carrying the energy and the specific angular momentum of the innermost stable circular orbit (ISO). This study thus provides estimates of the fractional increase of mass $\Delta M_{\rm BH}/M_{\rm BH,0}$ and spin $\Delta a/a_0$ during BH alignment (the subscript 0 refers to initial conditions), together with a sensible expression for the alignment time $t_{\rm al}$. In our context, we assume a continuous and coherent feeding of the accretion disc around the BH, at least for a time as long as the alignment time-scale $t_{\rm al}$. Thus, we consider an open system and we fix the orbital angular momentum direction $\hat{\boldsymbol{J}}_{\rm disc,out}$ at the outer edge of the disc.

In Section 2, we introduce key parameters and highlight our model assumptions. Section 3 surveys properties of steady-state warped discs and key scales associated to the Bardeen–Petterson effect; disc models with constant and power-law viscosity profile are explored for completeness. In Section 4, we describe the equations for the BH mass and spin evolution, and introduce the adiabatic approximation to solve these equations. In the same section, we also revisit the expression for the BH alignment time. Results are illustrated in Section 5; there we also explore the tendency to align in initially counter-rotating warped discs. Section 6 contains the discussion of the results and our conclusions.

2 INITIAL ASSUMPTIONS AND MAIN PARAMETERS

We consider a BH with spin $\boldsymbol{J}_{\rm BH}$, surrounded by a geometrically thin, standard Shakura–Sunyaev α-disc (e.g. Shakura & Syunyaev 1973; Frank, King & Raine 2002). The α-disc is initially misaligned relative to $\boldsymbol{J}_{\rm BH}$, i.e. the angular momentum unit vector of the disc at the outer edge is $\hat{\boldsymbol{J}}_{\rm disc,out} \neq \hat{\boldsymbol{J}}_{\rm BH}$; the relative inclination angle between the two unit vectors is $\theta_{\rm out}$.

Following Pringle (1992), we assume that the accretion disc has a high viscosity ($\alpha > H/R$, where H is the disc vertical scaleheight) so that perturbations propagate diffusively. We introduce two viscosity parameters, ν_1 and ν_2: ν_1 is the standard radial shear viscosity while ν_2 is the vertical share viscosity associated to the diffusion of vertical warps through the disc, due to Lense–Thirring precession. For ν_1, we adopt the α prescription

$$\nu_1 = \alpha H c_{\rm s}, \tag{2}$$

Table 1. Table of the coefficients α and f_{ν_2}.

α	f_{ν_2}
0.18	1.00
0.15	0.85
0.09	0.60
0.05	0.38

where $c_{\rm s}$ is the sound speed inside the accretion disc. It is still poorly understood which is the relation between the radial and the vertical viscosity, in particular, if $\nu_1 \sim \nu_2$ or $\nu_1 \ll \nu_2$. In order to simplify our discussion, we refer to the recent analysis of Lodato & Pringle (2007), and for ν_2 we take

$$\frac{\nu_2}{\nu_1} = \frac{f_{\nu_2}}{2\alpha^2}, \tag{3}$$

where f_{ν_2} (given in Table 1) is a coefficient determined in numerical simulations that accounts for non-linear effects.

The disc model is defined after specifying five free parameters (subscript 0 will be introduced to indicate initial values when mass and spin evolution is considered).

(1) The BH mass, $M_{\rm BH}$; we explore a mass range between $10^5 < M_{\rm BH} < 10^7\,{\rm M}_\odot$. For the BH mass, we introduce the dimensionless parameter M_6 as $M_{\rm BH} = M_6 \times 10^6\,{\rm M}_\odot$.

(2) The spin modulus, in terms of the dimensionless spin parameter a, which varies between $0 < a \leq 0.95$. We do not use the theoretical limit $a = 1$ because, if accretion is driven by magneto-rotational instabilities in a relativistic MHD disc, the final equilibrium spin due to continuous accretion is $a \approx 0.95$ (Gammie, Shapiro & McKinney 2004).

(3) The relative inclination angle $\theta_{\rm out}$ between the spin versor $\hat{\boldsymbol{J}}_{\rm BH}$ and the orbital angular momentum versor at the external edge of the accretion disc, $\hat{\boldsymbol{J}}_{\rm disc,out}$. This angle varies isotropically from 0 to π. In the following, however, we will confine this interval to (0, $\sim \pi/6$) in order to satisfy the used approximations.

(4) The viscosity parameter α which is assumed to vary between $10^{-2} \lesssim \alpha \lesssim 10^{-1}$ to bracket uncertainties (King, Pringle & Livio 2007). For our purposes, we selected values of α according to Lodato & Pringle (2007), as in Table 1. In this study, α is considered as a constant inside the disc.

(5) The accretion rate on to the BH, $\dot{M}$, is expressed in terms of the Eddington ratio $f_{\rm Edd} = L/L_{\rm Edd}$ and of the accretion efficiency η (where $L_{\rm Edd}$ is the Eddington luminosity): $\dot{M} = f_{\rm Edd} L_{\rm Edd}/(\eta c^2)$. We consider values of $f_{\rm Edd}$ in the interval $10^{-4} < f_{\rm Edd} < 1$ and compute η as a function of the BH spin modulus.

If the disc, warped in its innermost parts, is described to first order by the Shakura–Sunyaev α-model, both ν_1 and ν_2 follow a power law. If viscosities satisfy relation (3) and α is assumed to be constant, their exponent are equal:

$$\nu_1 = A_{\nu_1} R^\beta \qquad \text{and} \qquad \nu_2 = A_{\nu_2} R^\beta. \tag{4}$$

Following standard Shakura–Sunyaev disc solutions for external regions of an accretion disc (Frank et al. 2002), we have $\beta = 3/4$ and

$$A_{\nu_1} = 9.14 \times 10^6 \alpha_{0.1}^{4/5} M_6^{1/20} \left(\frac{f_{\rm Edd}}{\eta_{0.1}}\right)^{3/10} {\rm cm}^{5/4}\,{\rm s}^{-1},$$

$$A_{\nu_2} = \left(\frac{\nu_2}{\nu_1}\right) A_{\nu_1} = 50 f_{\nu_2} \alpha_{0.1}^{-2} A_{\nu_1}. \tag{5}$$

In equation (5), $\alpha_{0.1}$ and $\eta_{0.1}$ are the α coefficient and the BH radiative efficiency in unit of 0.1. f_{ν_2} is tabulated in Table 1 (Lodato & Pringle 2007).

3 WARPED ACCRETION DISC

3.1 The angular momentum content of discs: extended versus truncated discs

The dynamics of a fluid element in a misaligned disc around a spinning BH is given by the combination of three different motions: the Keplerian rotation around the BH; the radial drift, due to radial shear viscosity, and finally the Lense–Thirring precession, due to the gravitomagnetic field $\boldsymbol{H}_{\rm gm}$ generated by $\boldsymbol{J}_{\rm BH}$ (see e.g. Weinberg 1972; Thorne et al. 1986). In response to Lense–Thirring induced precession, viscous stresses in the disc acts rapidly to produce in the vicinity of the BH an axisymmetric configuration whereby adjacent fluid elements rotate in the equatorial plane of the spinning BH. The disc thus warps and the warp disturbance propagates diffusely (Papaloizou & Pringle 1983) in the disc.

As the Bardeen–Petterson effect modifies the inclination of the orbital plane of consecutive infinitesimal rings then the warped profile of the accretion disc can be described by the specific angular momentum density, $\boldsymbol{L}$, expressed as

$$\boldsymbol{L} = L\hat{\boldsymbol{l}} = \Sigma\Omega_{\rm K}R^2\hat{\boldsymbol{l}}, \tag{6}$$

where $\hat{\boldsymbol{l}}(R)$ is a unit vector indicating the local direction of the orbital angular momentum, L is the modulus, Σ is the surface density of the disc and $\Omega_{\rm K}$ the local Keplerian angular velocity. The angle describing the tilted disc is defined as

$$\theta(R) = \cos^{-1}[\hat{\boldsymbol{l}}(R)\cdot\hat{\boldsymbol{J}}_{\rm BH}], \tag{7}$$

so that $\hat{\boldsymbol{l}}(R)$ carries information of the warped structure of the accretion disc. The angular momentum of the accretion disc within radius R is given by

$$\boldsymbol{J}_{\rm disc}(R) = \int_{R_{\rm ISO}}^{R} 2\pi x\boldsymbol{L}(x){\rm d}x, \tag{8}$$

where the integration domain extends from the innermost stable orbit $R_{\rm ISO}$ out to R. In order to calculate the *total* disc angular momentum, we define an outermost radius, $R_{\rm out}$. For an extended disc with $R_{\rm out}\rightarrow\infty$, the disc angular momentum $\boldsymbol{J}_{\rm disc}$ always dominates over $\boldsymbol{J}_{\rm BH}$.

Real discs are likely to be truncated by their own self-gravity that becomes important at distances where the disc mass $M_{\rm disc}(R)\sim(H/R)M_{\rm BH}$ (see e.g. Pringle 1981; Frank et al. 2002; Lodato 2007). Outside the truncation radius, gas can be either turned into stars or expelled by winds from stars which do form (King & Pringle 2007; Levin 2007). Thus, we are led to define a disc outer edge as the distance where the Toomre parameter for stability, $Q = \kappa c_{\rm s}/(\pi G\Sigma)$ [where $\kappa^2 = R({\rm d}\Omega^2/{\rm d}R) + 4\Omega^2$], becomes less than unity, and the cooling time-scale of the clumping gas is less than its dynamical time-scale. When the Toomre parameter drops towards unity, the disc becomes unstable on a length-scale $\lambda = c_{\rm s}^2/(G\Sigma)$ (Polyachenko, Polyachenko & Strel'Nikov 1997; Levine et al. 2008); for a nearly Keplerian, Shakura–Sunyaev α-disc, this scale is much smaller than the disc radial dimension, and the cooling time of the associated perturbation is less or of the same order of its orbital period. Then, as long as the accretion disc can be described as a Shakura–Sunyaev disc,[1] the external radius can be defined from the condition $Q(R_{\rm out}) = 1$, so that

$$R_{\rm out} = 1.21\times10^5\alpha_{0.1}^{28/45}M_6^{-52/45}\left(\frac{f_{\rm Edd}}{\eta_{0.1}}\right)^{-22/45}R_{\rm S}, \tag{9}$$

where $R_{\rm S} = 2GM_{\rm BH}/c^2$ is the Schwarschild radius. At the outer edge of the disc, $\hat{\boldsymbol{l}}(R_{\rm out}) = \hat{\boldsymbol{J}}_{\rm disc,out}$ and $\theta(R_{\rm out}) = \theta_{\rm out}$.

Definitions (6) and (8) for $\boldsymbol{L}$ and $\boldsymbol{J}_{\rm disc}(R)$ hold for any disc profile. At first order, we can neglect details about the warped disc structure around $R_{\rm warp}$ assuming $\hat{\boldsymbol{l}}\approx(0,0,1)$, and estimate the modulus of the orbital angular momentum within radius R, $J_{\rm disc}(R)$, using Shakura–Sunyaev solutions for a flat disc. In this approximation, the surface density is $\Sigma_{\rm flat}\approx\dot{M}/(3\pi\nu_1)$ (see e.g. Pringle 1981; Frank et al. 2002) and

$$L(R)\approx\frac{\dot{M}}{3\pi\nu_1}\sqrt{GM_{\rm BH}R}. \tag{10}$$

Using equations (8) and (10), and expression (4) for ν_1 in the case of $\beta = 3/4$, the modulus of the disc angular momentum within R reads:

$$J_{\rm disc}(R) = \frac{8}{21}\frac{\dot{M}\sqrt{GM_{\rm BH}}}{A_{\nu_1}}R^{7/4}. \tag{11}$$

If expression (11) is estimated at the outer radius (9), the resulting dimensionless ratio between the disc and BH angular momenta is

$$\frac{J_{\rm disc}(R_{\rm out})}{J_{\rm BH}} = 7.3\,\alpha_{0.1}^{13/45}M_6^{-37/45}\left(\frac{f_{\rm Edd}}{\eta_{0.1}}\right)^{-7/45}a^{-1}. \tag{12}$$

3.2 Time-scales and warp radius

The time-dependent evolution of the disc is described by the continuity equation

$$R\frac{\partial\Sigma}{\partial t} + \frac{\partial}{\partial R}(v_{\rm R}\Sigma R) = 0, \tag{13}$$

where $v_{\rm R}$ is the radial component of the velocity vector, and by the equation of conservation of angular momentum. In presence of a gravitomagnetic field, for a geometrically thin disc characterized by the two viscosities ν_1 and ν_2, the equation reads (Pringle 1992):

$$\begin{aligned}\frac{\partial\boldsymbol{L}}{\partial t} &= -\frac{1}{R}\frac{\partial}{\partial R}(R\boldsymbol{L}v_{\rm R}) + \frac{1}{R}\frac{\partial}{\partial R}\left(\nu_1\Sigma R^3\frac{{\rm d}\Omega}{{\rm d}R}\hat{\boldsymbol{l}}\right)\\ &\quad+\frac{1}{R}\frac{\partial}{\partial R}\left(\frac{1}{2}\nu_2RL\frac{\partial\hat{\boldsymbol{l}}}{\partial R}\right) + \frac{2G}{c^2}\frac{\boldsymbol{J}_{\rm BH}\times\boldsymbol{L}}{R^3}.\end{aligned} \tag{14}$$

The last term is the Lense–Thirring precession term and the associated angular velocity is

$$\boldsymbol{\Omega}_{\rm LT}(R) = \frac{2G}{c^2}\frac{\boldsymbol{J}_{\rm BH}}{R^3}. \tag{15}$$

The time-dependent equation (14) describes the radial drift of matter and the diffusion of warping disturbances across the high-viscosity disc.

This equation introduces several key scales.

[1] This condition is fulfilled only for $(M_6\ f_{\rm Edd})/(\alpha_{0.1}\,\eta_{0.1})\gtrsim4.3$. If this condition is not satisfied, the gas temperature drops below $\sim10^4$ K, in the external region of the disc where Q is still greater than unity. The change in the opacity likely modifies the structure of the outer disc, and we cannot explicitly use (9). In this paper, we assume that the outer region is sufficiently extended to provide matter and angular momentum to the inner regions and use self-consistently the Shakura–Sunyaev model to describe the disc in regions where the gravitomagnetic interaction takes place.

(i) The viscous/accretion time-scale for radial drift, related to the angular momentum transport parallel to $\boldsymbol{J}_{\rm disc,out}$, $t_{\rm acc}(R)$. It can be seen as the time it takes for a fluid element at R to accrete on to the BH (see e.g. Pringle 1981). Considering equation (14), the balance between the advection term and the viscous term proportional to ν_1 (both on the right-hand side of equation 14) leads to an estimate of the accretion time:

$$t_{\rm acc}(R) \sim R^2/\nu_1. \tag{16}$$

According to equation (16), we can introduce the disc consumption time-scale $t_{\rm disc}$, a concept useful when considering transient, truncated discs, as the accretion time-scale at the outer radius:

$$t_{\rm disc} \sim t_{\rm acc}(R_{\rm out}) = 1.71\times10^6\alpha_{0.1}^{-1/45}M_6^{-11/45}\left(\frac{f_{\rm Edd}}{\eta_{0.1}}\right)^{-41/45}\ {\rm yr}. \tag{17}$$

(ii) The time-scale for warp propagation, related to the radial diffusion of gravitomagnetic perturbations that transport the component of the disc angular momentum lying in the plane of the disc; this scale is inferred from equation (14) considering the term proportional to ν_2,

$$t_{\rm BP}(R) \sim \frac{R^2}{\nu_2} \sim \left(\frac{\nu_1}{\nu_2}\right) t_{\rm acc}(R). \tag{18}$$

The physical interpretation of this time-scale has been recently investigated by solving numerically equation (14) for a thin disc (Lodato & Pringle 2006): starting at $t = 0$ with a flat disc misaligned relative to the fixed BH spin, $t \approx t_{\rm BP}(R)$ indicates the time it takes for the radial diffusion of the warp to reach radius R; on longer time-scale, the disc approaches a steady warped state.

(iii) The characteristic extension of the warp $R_{\rm warp}$, defined as the distance at which the Bardeen–Petterson time-scale $t_{\rm BP}(R)$ equals the Lense–Thirring precession time-scale $\Omega_{\rm LT}^{-1}$:

$$R_{\rm warp} = \frac{4GJ_{\rm BH}}{\nu_2 c^2}. \tag{19}$$

For power-law viscosity model, equations (1), (5) and (19) give

$$R_{\rm warp} = 476\alpha_{0.1}^{24/35}f_{\nu_2}^{-4/7}M_6^{4/35}\left(\frac{f_{\rm Edd}}{\eta_{0.1}}\right)^{-6/35}a^{4/7}R_{\rm S}. \tag{20}$$

The warp radius represents the division between the outer region for $R \gg R_{\rm warp}$, where the disc keeps its original inclination, given by $\hat{\boldsymbol{J}}_{\rm disc,out}$, and the inner region for $R \ll R_{\rm warp}$, where the disc aligns (or anti-aligns) its orbital angular momentum with the BH spin, $\hat{\boldsymbol{l}} \parallel \hat{\boldsymbol{J}}_{\rm BH}$. The warp radius fixes also the magnitude of the relevant Bardeen–Petterson time-scale, which reads

$$t_{\rm BP}(R_{\rm warp}) = 33.5\alpha_{0.1}^{72/35}f_{\nu_2}^{-12/7}M_6^{47/35}\left(\frac{f_{\rm Edd}}{\eta_{0.1}}\right)^{-18/35}a^{5/7}\ {\rm yr}. \tag{21}$$

If we define the function

$$\psi(R) \doteq \left|\frac{{\rm d}\hat{\boldsymbol{l}}}{{\rm d}R}\right| \tag{22}$$

and $R_{\rm BP}$ the radius where the disc is maximally deformed

$$\Psi \doteq \psi(R_{\rm BP}) = \max(\psi), \tag{23}$$

we expect that

$$R_{\rm BP} = n_{\rm BP}R_{\rm warp} \tag{24}$$

with $n_{\rm BP}$ of the order of unity. $R_{\rm BP}$ has two important properties: first, if it is the radius where the disc is maximally warped, i.e. where the diffusive propagation of vertical perturbations is more significant; secondly, it provides a reliable estimate of the distance from the BH where the gravitomagnetic interaction is stronger. From equation (14), this interaction is proportional to $(\boldsymbol{L}\times\boldsymbol{J}_{\rm BH})/R^3$: this term vanishes in the inner part of the disc ($R \ll R_{\rm BP}$) since the Bardeen–Petterson effect aligns $\boldsymbol{L}$ with $\boldsymbol{J}_{\rm BH}$, and also in the outer regions ($R \gg R_{\rm BP}$), due to the rapid decline with R. Accordingly, the region near $R_{\rm BP}$ (or equivalently $R_{\rm warp}$) is the only one significantly misaligned with $\boldsymbol{J}_{\rm BH}$.

3.3 Analytical solutions

In this section, we summarize the properties of the steady warped disc structure used to compute the joint evolution of the disc and the BH.

Following previous studies, we assume that the viscosity profiles are power laws with exponent β, as in equation (4), and explore two possible cases. In the first, we formally extend the Shakura–Sunyaev solution everywhere in the disc, i.e. $\nu_1 \propto R^\beta$ with $\beta = 3/4$, and ν_2 given by equation (3) (Martin et al. 2007). In the second case, we assume the viscosities to remain approximately constant everywhere in the disc (Scheuer & Feiler 1996). In order to compare the two models (cf. Martin et al. 2007), we impose the continuity of the viscosities at $R_{\rm BP}$ where the gravitomagnetic torque is most important.

Before solving equations (13) and (14), we introduce two appropriate reference frames. The first is the inertial reference frame $Oxyz$ referred to the outer disc; we can always rotate it so that its z-axis is parallel to the direction of $\hat{\boldsymbol{J}}_{\rm disc,out}$. The second reference frame is the not-inertial frame $O'x'y'z'$ referred to the BH spin, which is always centred to the BH and whose z'-axis is parallel to the BH time varying spin $\boldsymbol{J}_{\rm BH}$. If we use the adiabatic approximation then frame $O'x'y'z'$ can be approximated, with time t, as a sequence of frames, one for every quasi-stationary state of the system. The shape of the warped accretion disc is studied in the $O'\,x'\,y'\,z'$ frames and the Cartesian components of any vector $\boldsymbol{v}$ are there indicated as v'_x, v'_y, v'_z; $Oxyz$ is the natural frame to study the temporal evolution of the BH spin and here the Cartesian components of the previous vector are denoted as v_x, v_y, v_z.

For a stationary state, continuity equation (13) can be easily integrated introducing the accretion rate $\dot{M}$ as constant of integration:

$$R\Sigma v_{\rm R} = -\frac{\dot{M}}{2\pi}, \tag{25}$$

while the projection of equation (14) along $\hat{\boldsymbol{l}}$ reads:

$$\left(\frac{3}{2}\nu_1\frac{{\rm d}L}{{\rm d}R} - \frac{\dot{M}\sqrt{GM_{\rm BH}}}{4\pi\sqrt{R}}\right) + \frac{1}{2}R\nu_2 L\left|\frac{{\rm d}\hat{\boldsymbol{l}}}{{\rm d}R}\right|^2 = 0. \tag{26}$$

In the small deformation approximation (Scheuer & Feiler 1996), the warp is gradual and we can neglect the non-linear term, proportional to $|\partial\boldsymbol{l}/\partial R|^2$. Using the boundary condition $\Sigma(R_{\rm ISO}) = 0$, the integral of (26) is

$$L(R) = \frac{\dot{M}}{3\pi\nu_1}\sqrt{GM_{\rm BH}R}\left(1-\sqrt{\frac{R_{\rm ISO}}{R}}\right). \tag{27}$$

This means that, in this approximation scheme, the modulus of the angular momentum density for a warped accretion disc far from the horizon is the same as for a flat disc (equation 10).

Following Scheuer & Feiler (1996), we study the disc profile of the steady disc introducing the complex variable $W' = \hat{l}'_x + i\hat{l}'_y$ and considering the case $\theta_{\rm out} < \pi/2$. Using power-law viscosities according to (4), analytic solutions of equation (14) in the small

deformation approximation have been found by Martin et al. (2007):

$$W'_{\rm PL} = B\left(\frac{R}{R_{\rm warp}}\right)^{-\frac{1}{4}} \times K_{1/2(1+\beta)}\left[\frac{\sqrt{2}(1-i)}{(1+\beta)}\left(\frac{R}{R_{\rm warp}}\right)^{-\frac{1+\beta}{2}}\right], \quad (28)$$

where B is a complex constant of integration, depending on the boundary condition at the external edge, the subscript 'PL' is a reminder of the power-law viscosities and $K_{1/[2(1+\beta)]}$ is the modified Bessel function of the order of $1/[2(1+\beta)]$. In the particular case where we consider constant viscosities, i.e. $\beta = 0$, the solution can be written as

$$W'_{\rm C} = A\exp\left[-\sqrt{2}(1-i)\left(\frac{R}{R_{\rm warp}}\right)^{-\frac{1}{2}}\right], \quad (29)$$

where A is a complex constant of integration and the subscript 'C' is a reminder of the constant viscosity model (Scheuer & Feiler 1996). In this latter case, $n_{\rm BP}$ is calculated self-consistently, using the definition (24) and the prescription for constant viscosity evaluation at $R_{\rm BP}$; we find that, for every possible parameter set, $n_{\rm BP} \approx 0.42$. We note that W' (and so also ψ) depends on the radius R through the dimensionless ratio $R/R_{\rm warp}$ (Martin et al. 2007).

In Fig. 1, we plot the modulus of the gradient of $\hat{\boldsymbol{l}}$, $\psi(R)$, which is a local measure of the deformation degree of the disc, for a particular set of parameters and for three different angles, $\theta_{\rm out} = \pi/3$, $\pi/30$, $\pi/300$. The shape of ψ is similar for the two different disc profiles and for all the angles: there is a well-defined maximum near $R_{\rm warp}$, where we expect the disc to be more deformed. At radii smaller than $R_{\rm warp}$ and far from $R_{\rm warp}$, the disc is almost flat (note that the graph is logarithmic in both axes). For the constant viscosity (power-law) profile, the peak is at $R_{\rm BP} \approx 0.42R_{\rm warp}$ ($R_{\rm BP} \approx 0.38R_{\rm warp}$). In Fig. 1, we also see that a constant viscosity disc is less warped (since the maximum deformation is the smaller) than the power-law viscosity disc. The ratio between the maximum deformations in the power law versus constant viscosity is roughly a factor of 2, and it does not depend on the inclination angle (except for a scalefactor, approximately equal to the ratio between the corresponding angles).

3.4 Validity of the approximation

We calculated the warped disc profile under the small deformation approximation. We neglected second-order terms in equation (26) and found an analytic solution for $\boldsymbol{L}$; in order to verify the consistence of this approximation, we define χ_β as the ratio between the neglected term and the first term into the round brackets of (26), assuming to have a Keplerian disc with power-law viscosity profile with exponent β, like in equation (4). Considering equations (27) for L, we have $\mathrm{d}L/\mathrm{d}R \approx (1/2+\beta)(L/R)$ and then χ_β reads

$$\chi_\beta(R) = \frac{2}{3(\beta+1)}\frac{\nu_2}{\nu_1}\left|\frac{\mathrm{d}\boldsymbol{l}}{\mathrm{d}R}\right|^2 R^2. \quad (30)$$

Once we know the explicit solutions, the consistence of this approximation can be tested a posteriori calculating χ_β: the approximation is well satisfied if $\chi_\beta \ll 1$. From equation (30), χ_β can be expressed also as a function of $R/R_{\rm warp}$ and ψ:

$$\chi_\beta = \frac{2}{3(\beta+1)}\frac{\nu_2}{\nu_1}R_{\rm warp}^2\left(\frac{R}{R_{\rm warp}}\right)^2\psi^2\left(\frac{R}{R_{\rm warp}}\right). \quad (31)$$

Fig. 2 shows the function $\chi_{\beta=0}$ for constant viscosity profiles (dashed lines) and the function $\chi_{\beta=3/4}$ for power-law viscosity profiles (solid lines), for the same parameters as in Fig. 1.

The function χ_β exhibits a maximum, $(\chi_\beta)_{\rm max}$, around $R_{\rm warp}$. Far from $R_{\rm warp}$, the accuracy of the approximation increases, albeit slowly. The function χ_β is most sensitive to the inclination angle, as expected (note that Fig. 2 uses logarithmic axes).

In Fig. 3, we test the validity of the small deformation approximation plotting, in the BH mass versus $\theta_{\rm out}$ plane, the colour coded values of $(\chi_{\beta=0})_{\rm max}$, for different values of the viscosity parameter α (Table 1), using the constant viscosity profile model (we fix

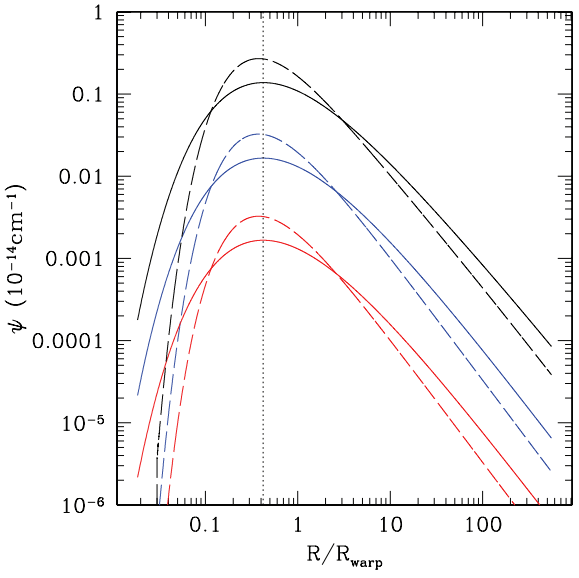

Figure 1. ψ as function of $R/R_{\rm warp}$, for $W'_{\rm C}$ (solid line) and $W'_{\rm PL}$ (dashed line) for different inclination angles: black lines correspond to $\theta_{\rm out} = \pi/3$, blue lines to $\pi/30$, red lines to $\pi/300$. The vertical black dotted line represents $R_{\rm BP}/R_{\rm warp} = 0.42$, the Bardeen–Petterson radius for constant viscosity profiles. The parameter set for the BH and the disc is given by $M_{\rm BH,0} = 10^6\,{\rm M}_\odot$, $a = 0.5$, $f_{\rm Edd} = 0.1$, $\alpha = 0.09$.

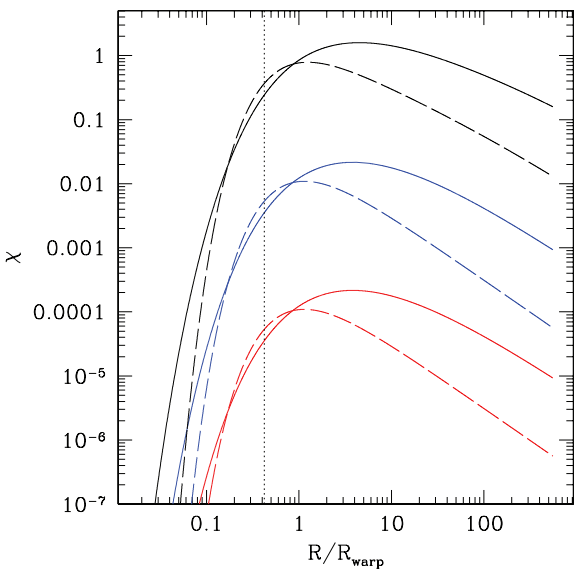

Figure 2. $\chi_{\beta=0}(R)$ (solid line) and $\chi_{\beta=3/4}$ (dashed lines) as functions of $R/R_{\rm warp}$ for different inclination angles. Black lines correspond to $\theta_{\rm out} = \pi/3$, blue ones to $\pi/30$, red ones to $\pi/300$; the vertical black dotted line represents $R_{\rm BP}/R_{\rm warp} = 0.42$, the Bardeen–Petterson radius for constant viscosity profiles. The parameter set for the BH and the disc is given by $M_{\rm BH,0} = 10^6\,{\rm M}_\odot$, $a = 0.5$, $f_{\rm Edd} = 0.1$, $\alpha = 0.09$.

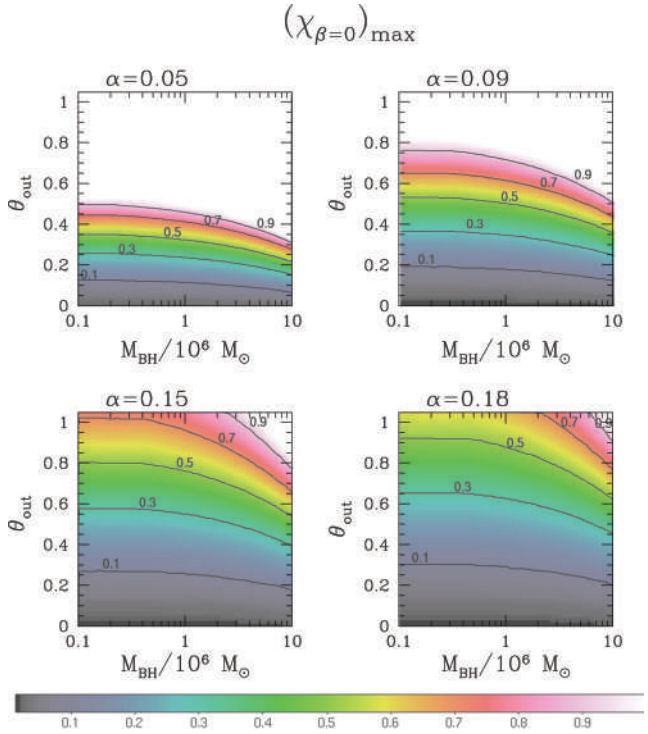

Figure 3. Colour-coded plot of $(\chi_\beta)_{max}$ in the θ_{out} versus M_{BH} plane, for four different α parameters: $\alpha = 0.05$ – top left-hand panel; $\alpha = 0.09$ – top right-hand panel; $\alpha = 0.15$ – bottom left-hand panel; $\alpha = 0.18$ – bottom right-hand panel. The disc has constant viscosity profiles, i.e. $\beta = 0$. The accretion rate is $f_{Edd} = 0.1$ and the spin parameter is $a = 0.9$.

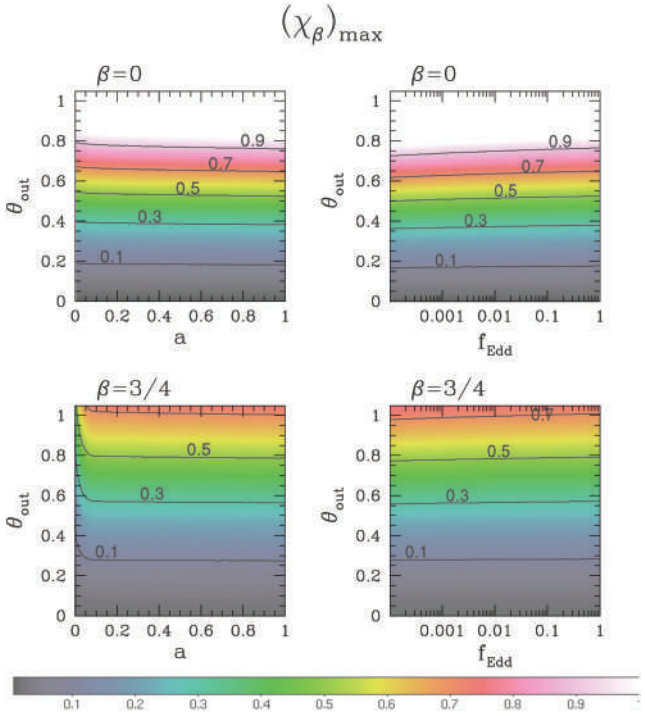

Figure 4. Left-hand panels: colour-coded plot of $(\chi_\beta)_{max}$ in the a versus θ_{out} plane, for $\alpha = 0.09$, $M_{BH} = 10^5\,M_\odot$ and $f_{Edd} = 0.1$. Right-hand panels: colour-coded plot of $(\chi_\beta)_{max}$ in the f_{Edd} versus θ_{out} plane, for $\alpha = 0.09$, $M_{BH} = 10^5\,M_\odot$ and $a = 0.9$. Top panels refer to constant viscosity profiles, bottom panels to power-law viscosity profiles.

$f_{Edd} = 0.1$ and $a = 0.9$). White zones represent the regions where $(\chi_{\beta=0})_{max} > 1$, i.e. where the small deformation approximation becomes invalid. $(\chi_{\beta=0})_{max}$ shows mainly a strong dependence on inclination angle θ_{out}, but also a weaker dependence on the BH mass which reveals that the small deformation approximation is less accurate for $M_{BH} \gtrsim 10^6\,M_\odot$ and increasing BH mass. Comparing different α values, the approximation is better satisfied for large viscosities parameters (i.e. $\alpha = 0.18$). We repeated the analysis for the power-law viscosity model that shows no significant differences in the parameters' dependence.

In Fig. 4, using the same colour conventions, we explored $(\chi_\beta)_{max}$ in the θ_{out} versus a (left-hand panels) and f_{Edd} versus θ_{out} (right-hand panels) planes, once we have fixed the viscosity parameter ($\alpha = 0.09$), the BH mass ($M_{BH} = 10^6\,M_\odot$) and $f_{Edd} = 0.1$ for the left-hand panels and $a = 0.9$ for the right-hand panels. For both constant ($\beta = 0$) and power-law ($\beta = 3/4$) models, the relative inclination angle is again the leading parameter gauging the goodness of the fit as the approximation depends very weakly on a and f_{Edd}.

4 BLACK HOLE EVOLUTION

4.1 Basic equations

In this section, we explore the equations for the BH evolution. The BH is accreting and its mass increases, from an initial value $M_{BH,0}$, according to

$$\frac{dM_{BH}}{dt} = \dot{M}\frac{E(R_{ISO})}{c^2}, \tag{32}$$

where $E(R_{ISO})$ is the energy per unit mass of a test particle at the innermost stable orbit. $E(R_{ISO})/c^2 = 1 - \eta(a)$ is related to the efficiency $\eta(a)$ that depends only on the spin parameter (Bardeen 1970; Bardeen, Press & Teukolsky 1972). Equation (32) introduces a natural time-scale for BH mass growth, known as Salpeter time t_S:

$$t_S = 4.5 \times 10^8 \frac{\eta}{f_{Edd}(1-\eta)}\ \mathrm{yr}. \tag{33}$$

As argued by Rees (1978) and shown by Thorne et al. (1986), there is a coupling between the BH spin and the angular momentum of the disc. Even though the disc is much less massive that the BH, the moving fluid elements perturb the Kerr metric and interact with the BH spin, causing spin *precession* and, if viscous dissipation is present, *alignment*. For an infinitesimal ring of inviscid matter with total angular momentum $\boldsymbol{J}_{ring}$, the BH spin precesses, following the equation

$$\frac{d\boldsymbol{J}_{BH}}{dt} = \frac{2G}{c^2}\frac{\boldsymbol{J}_{ring}}{R^3} \times \boldsymbol{J}_{BH}, \tag{34}$$

with a precession frequency

$$\Omega_{BH}^{precession} = \Omega_{LT}\frac{J_{ring}}{J_{BH}}. \tag{35}$$

Equation (34) can be extended to the case of an accretion disc to yield

$$\frac{d\boldsymbol{J}_{BH}}{dt} = \dot{M}\Lambda(R_{ISO})\hat{\boldsymbol{l}}(R_{ISO}) + \frac{4\pi G}{c^2}\int_{disc}\frac{\boldsymbol{L}(R) \times \boldsymbol{J}_{BH}}{R^2}dR. \tag{36}$$

The first contribution is due to accretion of matter at R_{ISO} where $\Lambda(R_{ISO})$ indicates the orbital angular momentum per unit mass carried by matter at ISO; the Bardeen–Petterson effect ensures that the direction of $\hat{\boldsymbol{l}}(R_{ISO})$ is parallel or antiparallel to $\hat{\boldsymbol{J}}_{BH}$, so that the accretion modifies only the spin modulus. As shown by Bardeen (1970), a variation of mass $\Delta M_{BH} = \sqrt{6}M_{BH,0}$ is necessary to

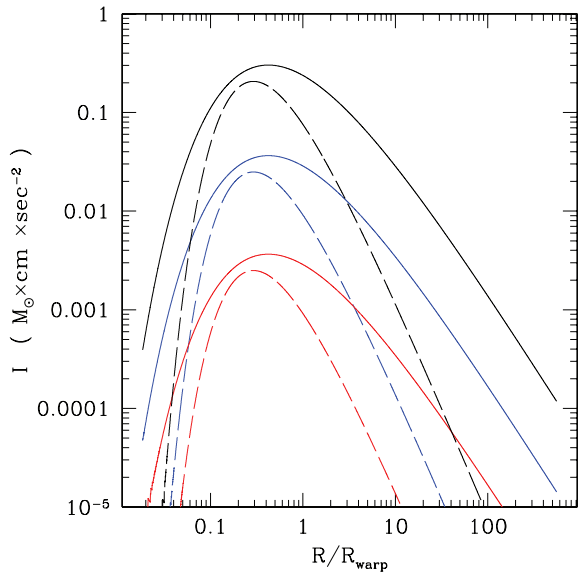

Figure 5. In this figure, we draw modulus of gravitomagnetic interaction term, I, as a function of radius normalized to warp radius, $R/R_{\rm warp}$. Disc profiles are obtained by BH with $M_{\rm BH} = 10^6\,{\rm M}_\odot$ and $a = 0.5$, and accretion disc with $f_{\rm Edd} = 0.1$ and $\alpha = 0.09$. Solid (dashed) lines refer to constant (power-law) viscosity profiles; black lines to $\theta_{\rm out} = \pi/3$, blue lines to $\theta_{\rm out} = \pi/30$, red lines to $\theta_{\rm out} = \pi/300$.

pass from a Schwarzschild BH ($a = 0$) to an extreme Kerr BH ($a = 1$), while spin flip of π, due only to accretion on an initially extreme Kerr BH, needs $\Delta M_{\rm BH} = 3\,M_{\rm BH,0}$. So, the spin accretion time-scale for the spin modulus is of the same order of the mass accretion time-scale $t_{\rm S}$. The second term in equation (36) describes the gravitomagnetic interaction between the rotating viscous disc and the BH spin vector. This term modifies only the *spin direction* of the BH in order to conserve the total angular momentum of the system. Under the working hypothesis that the disc is continually fed by matter carrying the same angular momentum (see Section 6 for a critical discussion), the BH aligns its spin $\boldsymbol{J}_{\rm BH}$ in the direction of $\hat{\boldsymbol{J}}_{\rm disc,out}$. Alignment implies that $\theta_{\rm out}(t) = \cos^{-1}[\hat{\boldsymbol{J}}_{\rm BH}(t)\cdot\hat{\boldsymbol{J}}_{\rm disc,out}]$ goes to 0 with time. Fig. 5 shows the function I defined as the modulus of the integral kernel of equation (36)

$$I(R) = \frac{4\pi G}{c^2}\frac{L(R)J_{\rm BH}\sin[\theta(R)]}{R^2} \tag{37}$$

as a function of $R/R_{\rm warp}$, for different value of $\theta_{\rm out} = \pi/3$, $\pi/30$, $\pi/300$, where $\theta(R)$ is computed along the profile of the steady warped disc of equations (28) and (29). The function I, similarly to ψ (defined in equation 22), peaks near $R_{\rm warp}$. Contrary to ψ, power-law viscosity profiles have lower peaks, compared with constant viscosity profiles. This figure indicates also that the BH–disc gravitomagnetic interaction is spread over a relatively small region of the disc around the warp radius; the characteristic spreading length, which is slightly larger for constant viscosity profiles, is usually of a few warp radii.

4.2 Alignment time

In this section, we want to give simple estimations for the alignment and the precession time-scales, starting from equation (36).

Assuming BH mass and spin modulus variations due to accretion to be small compared with gravitomagnetic effects during the alignment, we neglect the term proportional to $\Lambda(R_{\rm ISO})$ in (36); if BH spin aligns and precesses, left-hand side of (36) can be estimated introducing a characteristic gravitomagnetic time-scale $\tau_{\rm gm}$ as

$$\left|\frac{{\rm d}\boldsymbol{J}_{\rm BH}}{{\rm d}t}\right| \sim \frac{|\Delta\boldsymbol{J}_{\rm BH}|}{\tau_{\rm gm}} \sim \frac{J_{\rm BH}\sin\theta_{\rm out,0}}{\tau_{\rm gm}},$$

and the integral on the right-hand side as

$$\left|\frac{4\pi G}{c^2}\int_{\rm disc}\frac{\boldsymbol{L}(R)\times\boldsymbol{J}_{\rm BH}}{R^2}{\rm d}R\right| \sim \frac{4\pi G}{c^2}\frac{L(R_{\rm warp})J_{\rm BH}\sin\theta_{\rm out}}{R_{\rm warp}}$$

since the bulk of the gravitomagnetic interaction occurs around $R_{\rm warp}$. Equating these two expressions and using equation (27) for the specific angular momentum density modulus, we obtain

$$\tau_{\rm gm} \sim \frac{3}{4}\frac{c\nu_1(R_{\rm warp})}{G\dot{M}}\sqrt{\frac{R_{\rm warp}}{R_{\rm S}}}. \tag{38}$$

Using equations (19) and (11) which imply $\dot{M}\sqrt{GM_{\rm BH}}/\nu_1(R_{\rm warp}) \approx (21/8)\,J_{\rm disc}(R_{\rm warp})\,R_{\rm warp}^{-5/2}$, the gravitomagnetic scale $\tau_{\rm gm}$ can be written in terms of the Bardeen–Petterson warp time-scale (equation 18):

$$\tau_{\rm gm} \sim \frac{4\sqrt{2}}{7}\frac{J_{\rm BH}}{J_{\rm disc}(R_{\rm warp})}t_{\rm BP}(R_{\rm warp}) \tag{39}$$

and also in term of the accretion time-scale (equation 16)

$$\tau_{\rm gm} \sim \frac{4\sqrt{2}}{7}\frac{\nu_1}{\nu_2}\frac{J_{\rm BH}}{J_{\rm disc}(R_{\rm warp})}t_{\rm acc}(R_{\rm warp}), \tag{40}$$

where $J_{\rm disc}(R_{\rm warp})$ is the disc angular momentum modulus within the warp radius, estimated by (11). Finally, considering equations (11) and (16) for $t_{\rm acc}$ together with the expression for the spin modulus and Schwarzschild radius, $\tau_{\rm gm}$ of expression (40) can be rearranged as

$$\tau_{\rm gm} \sim \frac{3}{2}\,a\,\frac{\nu_1}{\nu_2}\,\frac{M_{\rm BH}}{\dot{M}}\sqrt{\frac{R_{\rm S}}{R_{\rm warp}}}. \tag{41}$$

Since the disc carries very little angular momentum at the warp radius, from equation (39) $\tau_{\rm gm} \gg t_{\rm BP}$, always. The gravitomagnetic BH–disc interaction causes BH spin precession and alignment at the same time, and then introduces two scales related with $\tau_{\rm gm}$, the *precession* and the *alignment* time-scales, $t_{\rm prec}$ and $t_{\rm al}$, respectively. We separate their relative importance following Martin et al. (2007) results, and define the parameter μ, so that

$$t_{\rm al} = \frac{\tau_{\rm gm}}{\cos\mu}, \qquad t_{\rm prec} = \frac{\tau_{\rm gm}}{\sin\mu}. \tag{42}$$

The exact value of μ depends on the viscosity profile, and can be estimated either analytically (Martin et al. 2007) or numerically as in this paper. Initially, we assume alignment and precession to have the same time-scale, $\cos\mu = \sin\mu = \sqrt{2}/2$ according to Scheuer & Feiler (1996). Substituting expressions (5) for the viscosities, (20) for the warp radius, and (38) for $\tau_{\rm gm}$ in (42), the alignment time reads

$$t_{\rm al} = 1.13\times10^5\alpha_{0.1}^{58/35}f_{\nu_2}^{-5/7}M_6^{-2/35}\left(\frac{f_{\rm Edd}}{\eta_{0.1}}\right)^{-32/35}a^{5/7}\,{\rm yr}. \tag{43}$$

The time-scale $t_{\rm al}$ increases with a, indicating that a rapidly rotating Kerr BH offers some resistance before changing its direction. Interestingly, the alignment time-scale does not depend on the initial inclination $\theta_{\rm out,0}$ since a more inclined configuration implies more pronounced disc deformations and stronger mutual gravitomagnetic interactions (as also shown in Figs 1 and 5). $t_{\rm al}$ has a weak dependence on the BH mass and scales nearly as $\dot{M}^{-1}$: a higher accretion rate implies a higher angular momentum density $\boldsymbol{L}(R)$ and thus a

stronger gravitomagnetic coupling. We also note that, apart from numerical factors of order unity, this time-scale is consistent with the alignment scales found by Scheuer & Feiler (1996), Natarajan & Pringle (1998), Natarajan & Armitage (1999) and Martin et al. (2007).

4.3 The adiabatic approximation

In Sections 3.2 and 4.1, we described the equations governing the evolution of a warped accretion disc around a fixed BH, and the evolution of an accreting Kerr BH in gravitomagnetic interaction with its accretion disc. The BH and the accretion disc evolve contemporary and their evolution is coupled, so that we can solve simultaneously equations (13) and (14) for a Keplerian disc and (32) and (36) for the accreting and precessing BH.

In this paper, we solve these coupled equations using the *adiabatic* approximation that separates the rapid temporal evolution of the warped disc from the longer temporal evolution of the BH. Equations are integrated starting from given initial conditions: at $t = 0$, the BH spin $\hat{\boldsymbol{J}}_{\rm BH}$ is inclined with respect to $\hat{\boldsymbol{J}}_{\rm disc,out}$ by an angle $\theta_{\rm out,0}$ and the warped disc profile is described by a quasi-stationary profile $\boldsymbol{L}\ (R, t = 0)$; $M_{\rm BH,0}$ and $\boldsymbol{J}_{\rm BH,0}$ are the initial BH mass and spin.

In order to justify this approximation scheme, we survey the BH and disc time-scales, as functions of $M_{\rm BH}$ and $f_{\rm Edd}$, for two selected values of the viscosity and spin parameter: $\alpha = 0.15$ and $a = 0.9$. In Figs 6 and 7, we draw in the $M_{\rm BH}$–$f_{\rm Edd}$ plane lines of constant $t_{\rm BP}(R_w)/t_{\rm al}$ and $t_{\rm S}/t_{\rm al}$ ratios. The comparison between the different time-scales lead to the following hierarchy of time-scales:

$$t_{\rm BP}(R_{\rm warp}) \ll t_{\rm al} \ll t_{\rm S}. \tag{44}$$

Then, in the adiabatic approximation, the disc transits through a sequence of warped states over the shortest time-scale $t_{\rm BP}(R_{\rm warp})$ while, on the longer time-scale $t_{\rm al}$, the BH aligns its spin to $\hat{\boldsymbol{J}}_{\rm disc,out}$, and modifies a little its spin modulus and mass due to accretion. Considering one of these disc quasi-steady-states, initially at time t, after a time gap $\delta t \sim t_{\rm BP}(R_{\rm warp})$ the BH mass and spin $\boldsymbol{J}_{\rm BH}$ are

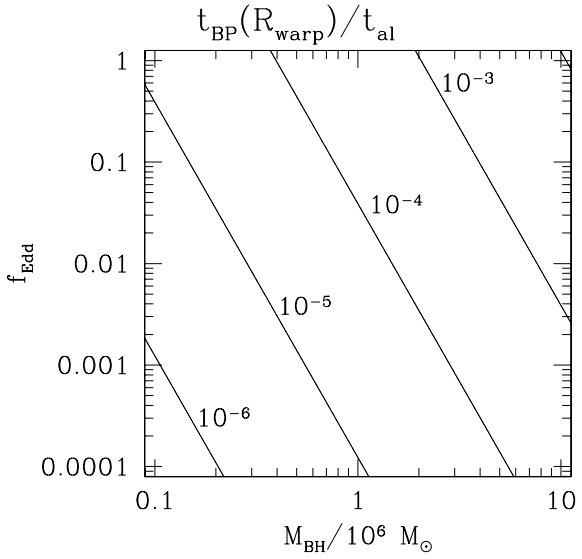

Figure 6. In the $M_{\rm BH}$ versus $f_{\rm Edd}$ plane, we draw lines of constant $t_{\rm BP}(R_{\rm warp})/t_{\rm al}$ ratio for a BH with $a = 0.9$ and an accretion disc with $\alpha = 0.09$.

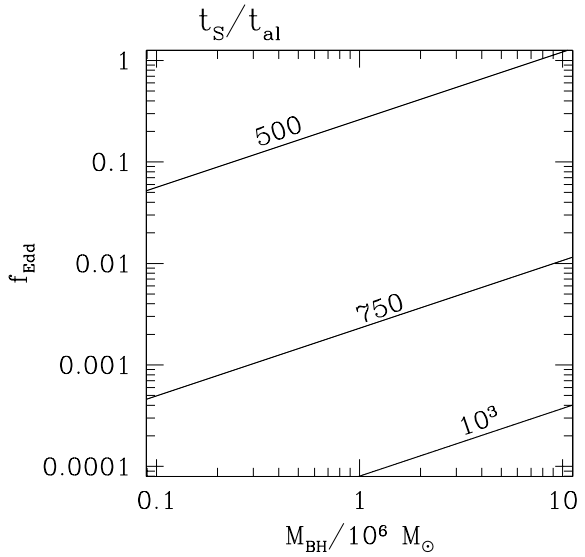

Figure 7. In the $M_{\rm BH}$ versus $f_{\rm Edd}$ plane, we draw lines of constant $t_{\rm S}/t_{\rm al}$ ratio for a BH with $a = 0.9$ and an accretion disc with $\alpha = 0.09$.

updated according to

$$\begin{cases} M_{\rm BH}[t + t_{\rm BP}(R_{\rm warp})] = M_{\rm BH}(t) + \delta M_{\rm BH} \\ \boldsymbol{J}_{\rm BH}[t + t_{\rm BP}(R_{\rm warp})] = \boldsymbol{J}_{\rm BH}(t) + \delta \boldsymbol{J}_{\rm BH} \end{cases} \tag{45}$$

and these variations produce a new quasi-stationary warped state at $t + t_{\rm BP}(R_{\rm warp})$, $\boldsymbol{L}[R, t + t_{\rm BP}(R_{\rm warp})]$.

For the BH mass variation $\delta M_{\rm BH}$, we integrate equation (32) from t to $t + t_{\rm BP}(R_{\rm BP})$:

$$\delta M_{\rm BH} \approx \dot{M} \frac{E(R_{\rm ISO})}{c^2} t_{\rm BP}(R_{\rm BP}), \tag{46}$$

where $R_{\rm ISO}$ is the last innermost stable orbit associated with the current value of $a(t)$.

For the spin variation, we need to integrate equation (36) that includes the two different and coupled contributions due to accretion and gravitomagnetic interaction; if $\delta M_{\rm BH}$ and $\delta \boldsymbol{J}_{\rm BH}$ are small on the time-scale $t_{\rm BP}(R_{\rm BP})$, to first order the two contributions decouple and they can be integrated separately:

$$(\delta J_{\rm BH})_{\rm acc} \approx \dot{M} \Lambda(R_{\rm ISO}) t_{\rm BP}(R_{\rm BP}), \tag{47}$$

$$(\delta \boldsymbol{J}_{\rm BH})_{\rm gm} \approx \frac{4\pi G}{c^2} t_{\rm BP}(R_{\rm BP}) \int_{\rm disc} \frac{\boldsymbol{L}(R, t) \times \boldsymbol{J}_{\rm BH}(t)}{R^2} {\rm d}R, \tag{48}$$

where $(\delta J_{\rm BH})_{\rm acc}$ is due to accretion and changes only the spin modulus while $(\delta \boldsymbol{J}_{\rm BH})_{\rm gm}$ is due to gravitomagnetic interaction and changes only the spin direction. After the interval $t_{\rm BP}(R_{\rm BP})$, the angular momentum of (45) is updated according to this rule:

$$\boldsymbol{J}_{\rm BH}[t + t_{\rm BP}(R_{\rm warp})] = \left[\boldsymbol{J}_{\rm BH}(t) + (\delta \boldsymbol{J}_{\rm BH})_{\rm gm}\right] \times \frac{J_{\rm BH}(t) + (\delta J_{\rm BH})_{\rm acc}}{J_{\rm BH}(t)}. \tag{49}$$

This procedure can be repeated iteratively on a time-scale $t_{\rm al}$ to study the coupled evolution of $\boldsymbol{L}(R, t)$, $\boldsymbol{J}_{\rm BH}$ and $M_{\rm BH}$ during the alignment process.

5 SPIN ALIGNMENT

5.1 Set up

In this section, we study the coupled evolution of the BH and warped accretion disc using the approximation scheme described in the

previous section, in order to infer the evolution of $M_{\rm BH}$ and $\boldsymbol{J}_{\rm BH}$ as a function of time, in response to the gravitomagnetic interaction and matter accretion.

At $t = 0$, the outer disc, extending up to a radius $R_{\rm out}$, defines the fixed reference frame $Oxyz$. In this frame, the external edge of the disc lies in the x, y plane and the orbital angular momentum at $R_{\rm out}$ is

$$[L_x(R_{\rm out}), L_y(R_{\rm out}), L_z(R_{\rm out})] = L(R_{\rm out})(0, 0, 1) \tag{50}$$

while the BH spin is initially inclined of $\theta_{\rm out,0}$ with respect to the z-axis:

$$(J_{{\rm BH},x}, J_{{\rm BH},y}, J_{{\rm BH},z}) = J_{\rm BH}(\sin\theta_{\rm out,0}, 0, \cos\theta_{\rm out,0}). \tag{51}$$

If at $t \neq 0$ we know the components of $\boldsymbol{J}_{\rm BH}$ in the fixed reference frame $Oxyz$ there is always a rotated reference frame $Ox'y'z'$ where $\boldsymbol{J}_{\rm BH}$ is along the new z'-axis (see also the discussion about reference frames of Section 3.3). The two reference frames are related by a rotation $\mathcal{R}$, which depends only on the components $J_{{\rm BH},x}$, $J_{{\rm BH},y}$, $J_{{\rm BH},z}$ of $\boldsymbol{J}_{\rm BH}(t)$ in the fixed reference frame. If $\mathcal{R}_{ij}$ is the matrix associated with this rotation, we can easily find the components of $\boldsymbol{J}_{\rm BH}(t)$ and $\boldsymbol{L}$ $(R_{\rm out}, t)$ in the rotated frame:

$$J'_{{\rm BH},i}(t) = \mathcal{R}_{ij} J_{{\rm BH},j}(t) \Rightarrow J'_{\rm BH}(t) = [0, 0, J_{\rm BH}(t)],$$
$$L'_i(R_{\rm out}, t) = \mathcal{R}_{ij} L_j(R_{\rm out}, t). \tag{52}$$

As shown by Scheuer & Feiler (1996) for the constant viscosity profile and Martin et al. (2007) for the power-law viscosity profile, in this special rotated frame of reference it is possible to calculate analytically the expression of the gravitomagnetic torque, using equation (48):

$$(\delta J'_{{\rm BH},x} + i\delta J'_{{\rm BH},y})_{\rm gm} = \left[-i\frac{4\pi G J_{\rm BH}(t)}{c^2}\int_{\rm disc}\frac{L(R,t)W'(R,t)}{R^2}{\rm d}R\right] t_{\rm BP}(R_{\rm warp}), \tag{53}$$

where $L(R, t)$ is given by (27) and $W'(R, t)$ by (29) or (28). The analytic expressions of the gravitomagnetic torques for the two viscosity profiles are reported in the Appendix. From the torques, it is possible to find the values of the spin variations $(\delta J'_{{\rm BH},x})_{\rm gm}$, $(\delta J'_{{\rm BH},y})_{\rm gm}$ and $(\delta J'_{{\rm BH},z})_{\rm gm}$ in this rotated reference frame. Finally, in order to know their expressions in our fixed reference frame $Oxyz$, we have to rotate them back, using the inverse rotation $\mathcal{R}^{-1}$

$$(\delta J_{{\rm BH},i})_{\rm gm} = (\mathcal{R}^{-1})_{ij}(\delta J'_{{\rm BH},j})_{\rm gm}. \tag{54}$$

Once we know the spin variations due to gravitomagnetic coupling, the modulus variation can be calculated from equation (47) and the global spin variation from equation (49).

5.2 Results

We computed, within the adiabatic approximation, the joint evolution of the BH mass and spin during the process of alignment under the assumption that matter is corotating with the BH. We iterated equations (46) and (49), from the initial conditions (50) and (51), recording the updated values of $M_{\rm BH}$, a and of the relative inclination angle $\theta_{\rm out}$ every snapshot of time $\delta t \sim t_{\rm BP}(R_{\rm warp})$. We initially choose a spinning BH with $M_{\rm BH} = 10^6\,{\rm M}_\odot$ and $a = 0.5$, and an accretion disc with $\dot{M} = 0.1\dot{M}_{\rm Edd}$, $\alpha = 0.09$; both power-law and constant viscosity profiles are considered. Three initial relative inclination angles of $\theta_{\rm out,0} = \pi/3, \pi/6, \pi/30$ have been tested. Fig. 8 shows as a function of time the inclination angle $\theta_{\rm out}(t)$ and the two components of the BH spin unit vector in the plane Oxy; red

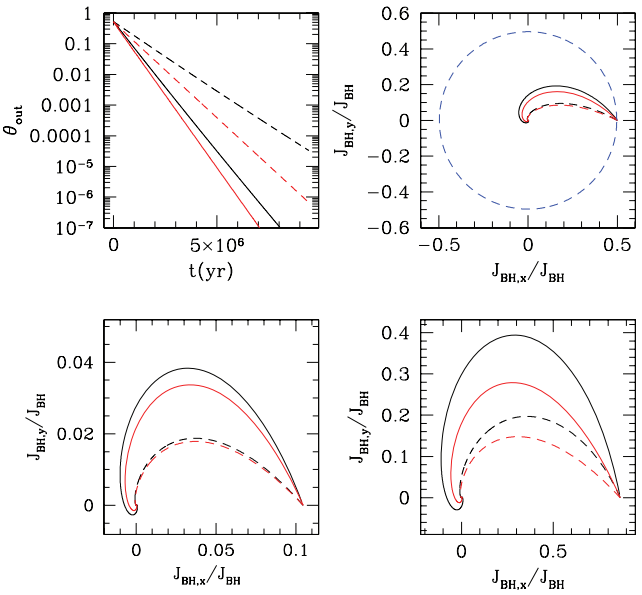

Figure 8. Results for precession and alignment processes. Black lines refer to our result while red lines refer to results published by Martin et al. (2007); solid lines (dashed lines) refer to constant (power-law) viscosity profile. Top left-hand panel represents temporal evolution of relative inclination angle $\theta_{\rm out}$ while top right shows evolution of $J_{\rm BH,x}/J_{\rm BH}$ against $J_{\rm BH,y}/J_{\rm BH}$, both for an initial BH with $M_{\rm BH,0} = 10^6\,{\rm M}_\odot$, $a_0 = 0.5$ and an accretion disc with $f_{\rm Edd} = 0.1$ and $\alpha = 0.09$, with $\theta_{\rm out,0} = \pi/6$. Blue dashed line represents the evolution of the spin components for a pure precession motion around $\hat{\boldsymbol{J}}_{\rm disc,out} \,||\, \hat{z}$. In bottom left-hand (right-hand) panel, we represent evolution of $J_{\rm BH,x}/J_{\rm BH}$ against $J_{\rm BH,y}/J_{\rm BH}$ for an initial relative inclination angle $\theta_{\rm out,0} = \pi/30$ ($\theta_{\rm out,0} = \pi/3$), for an initial BH with $M_{\rm BH,0} = 10^6\,{\rm M}_\odot$, $a_0 = 0.5$ and an accretion disc with $f_{\rm Edd} = 0.1$ and $\alpha = 0.09$.

lines refer to the analytic solutions given by Martin et al. (2007). As shown in top left-hand panel of Fig. 8, the relative inclination angle $\theta_{\rm out}$ decreases exponentially with time on the scale $t_{\rm al}$ and the decrease is more rapid for the constant viscosity disc (solid line).

The BH spin aligns with the external disc and precesses, as illustrated in the top-right panel, where we compare also the actual evolution of the spin versor with a pure precessional motion (blue dashed line). Our results are only qualitatively consistent with Martin's results; in our calculations, the alignment process appears to be less efficient and the spin precession more pronounced. The difference between our results and Martin's analytical solutions arises from three facts: (i) we included mass and spin modulus evolution; (ii) Martin et al. neglected to carry out the rotation connecting the BH reference frame $O'x'y'z'$ to the disc frame $Oxyz$; (iii) for constant viscosity profile, we evaluate ν_1 and ν_2 from equation (5) at the Bardeen–Petterson radius, $R_{\rm BP} \approx 0.4R_{\rm warp}$, while Martin et al. evaluate them at the warp radius, $R_{\rm warp}$. For an initially not very inclined BH spin, the difference tends to disappear, because the rotation matrix nears the identity matrix. However, for large $\theta_{\rm out,0}$ the discrepancy becomes more important (see e.g. bottom panels of Fig. 8).

Fig. 9 shows the evolution of $\theta_{\rm out}$ and a as functions of time and of the increasing BH mass, for an initial BH with $M_{\rm BH,0} = 10^6\,{\rm M}_\odot$, $\theta_{\rm out,0} = \pi/6$ and spin parameter $a_0 = 0.5$, and for $f_{\rm Edd} = 1$, 0.1 and 0.01. Both constant and power-law viscosity profiles are explored, always with viscosity parameter $\alpha = 0.09$. Alignment is a process that shows a strong dependence on the accretion rate: for the constant (power-law) viscosity model, the time necessary to reduce the relative inclination angle by a factor of 100 varies

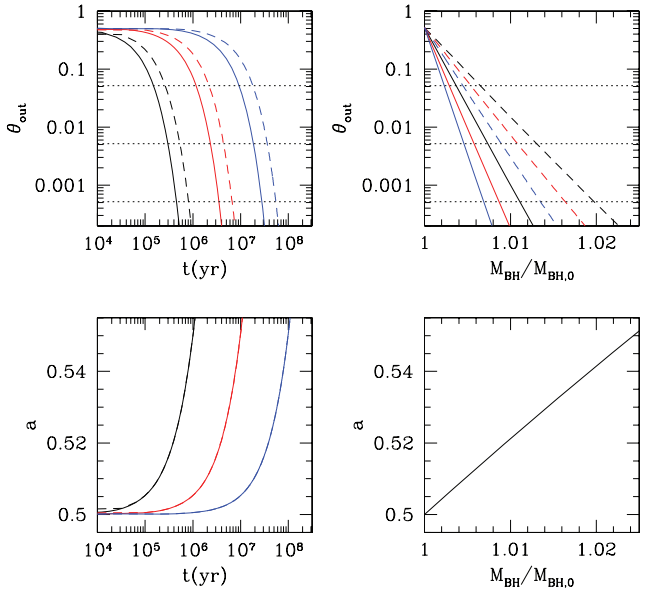

Figure 9. Coupled evolution of the relative inclination angle $\theta_{\rm out}$, BH mass $M_{\rm BH}$ and spin parameter a. Solid (dashed) lines refer to constant (power-law) viscosity profile. Black lines to $f_{\rm Edd} = 1$, red lines to $f_{\rm Edd} = 0.1$, blue lines to $f_{\rm Edd} = 0.01$. Dotted horizontal lines which appear in top panels represent angles $\theta_{\rm out}/\theta_{\rm out,0} = 10^{-1}, 10^{-2}, 10^{-3}$. Initial configuration: $M_{\rm BH,0} = 10^6\,{\rm M}_\odot$, $a_0 = 0.5$, $f_{\rm Edd} = 0.1$ and $\alpha = 0.09$, with $\theta_{\rm out,0} = \pi/6$.

from 3.0×10^5 yr (5.3×10^5 yr) for $f_{\rm Edd} = 1$ to 1.86×10^7 yr (3.63×10^7 yr) for $f_{\rm Edd} = 0.01$. During this alignment time, the BH has increased its mass by a small fraction, between 0.74 per cent (1.30 per cent) for $f_{\rm Edd} = 1$ and 0.46 per cent (0.89 per cent) for $f_{\rm Edd} = 0.01$. The spin parameter a increases due to accretion, but only by a small amount, between 3.13 per cent (5.47 per cent) for $f_{\rm Edd} = 1$ and 1.96 per cent (3.79 per cent) for $f_{\rm Edd} = 0.01$.

In Table 2, we summarize the results of Fig. 9. There, we compare also the time Δt necessary to decrease the initial inclination angle by a given amount, with $t_{\rm al}$ estimated from equation (43): the values of the time Δt are consistent with the interpretation of $t_{\rm al}$ as e-folding time. For constant viscosity profiles, a closer match of $t_{\rm al}$ with the numerical outcomes requires $(\cos\mu)_{\rm C} \approx 0.78$ instead of $\sqrt{2}/2$, and $(\cos\mu)_{\rm PL} \approx 0.41$ for power-law viscosity profiles (subscripts C and PL simply remind that for different viscosity prescriptions we found different $\cos\mu$ values). Then, the ratios between the precession and the alignment time-scales are $(t_{\rm prec}/t_{\rm al})_{\rm C} = 0.81$ and $(t_{\rm prec}/t_{\rm al})_{\rm PL} = 2.2$. These results are still qualitatively consistent with Martin et al. (2007), who have shown that both $t_{\rm al}$ and $t_{\rm prec}/t_{\rm al}$ increase with the exponent β of the viscosity profile; small quantitative differences are due to different assumptions and different calculations methods. Finally, we note that the scaling of Δt with $f_{\rm Edd}$ is in good agreement with estimation (43).

5.3 Exploring the parameter space

Here, we explore more systematically how the fractional increases of $M_{\rm BH}$ and a, and the alignment time vary with initial mass $M_{\rm BH,0}$, spin a_0, $f_{\rm Edd}$ and α, for both constant and power-law viscosity profiles, fixing $\theta_{\rm out,0} = \pi/6$. The evolution is followed until $\theta_{\rm out}$ has decreased by a factor of 100; we define as $\Delta t_{\theta_0 \to \theta_0/100}$ the corresponding 'alignment' time, computed self-consistently. We also infer from the numerical model the relative growths of BH mass $\Delta M_{\rm BH}/M_{\rm BH,0}$ and spin parameter $\Delta a/a_0$ during $\Delta t_{\theta_0 \to \theta_0/100}$.

Figs 10 and 11 show the weak dependence of the alignment time $\Delta t_{\theta_0 \to \theta_0/100}$ on the initial BH mass $M_{\rm BH,0}$, and of the relative

Table 2. Summary of our parameters and results for the corotating case; we consider viscosity coefficient $\alpha = 0.09$ and initial inclination angle $\theta_{\rm out,0} = \pi/6$, both for constant (C) and power-law (PL) viscosity profiles (VP).

VP	$f_{\rm Edd}$	$\theta_{\rm out}/\theta_{out,0}$	Δt (10^6 yr)	$\Delta t/t_{\rm al}$	$\Delta M_{\rm BH}/M_{\rm BH,0}$ (in units of 10^{-2})	$\Delta a/a_0$ (in units of 10^{-2})
C	1	10^{-1}	0.15	2.2	0.67	1.57
		10^{-2}	0.30	4.4	0.74	3.13
		10^{-3}	0.45	6.6	1.11	4.69
	0.1	10^{-1}	1.12	2.0	0.29	1.24
		10^{-2}	2.33	4.2	0.58	2.46
		10^{-3}	3.52	6.3	0.87	3.68
	0.01	10^{-1}	9.28	2.0	0.23	0.99
		10^{-2}	18.6	4.1	0.46	1.96
		10^{-3}	27.9	6.1	0.68	2.94
PL	1	10^{-1}	0.26	3.8	0.65	2.77
		10^{-2}	0.53	7.8	1.30	5.49
		10^{-3}	0.81	11.9	1.98	8.20
	0.1	10^{-1}	2.18	3.9	0.54	2.30
		10^{-2}	4.39	7.9	1.08	4.57
		10^{-3}	6.64	11.9	1.64	6.84
	0.01	10^{-1}	18.1	3.9	0.45	1.91
		10^{-2}	36.3	7.9	0.89	3.79
		10^{-3}	54.7	11.9	1.35	5.67

Note. The initial BH has $M_{\rm BH,0} = 10^6\,{\rm M}_\odot$ and $a_0 = 0.5$. Accretion rate $f_{\rm Edd}$ varies over three orders of magnitude and we record times needed to decrease the relative inclination angle of a factor of 10, 100 or 1000, comparing it with estimated alignment time-scale (equation 43); we also report mass and spin relative variations.

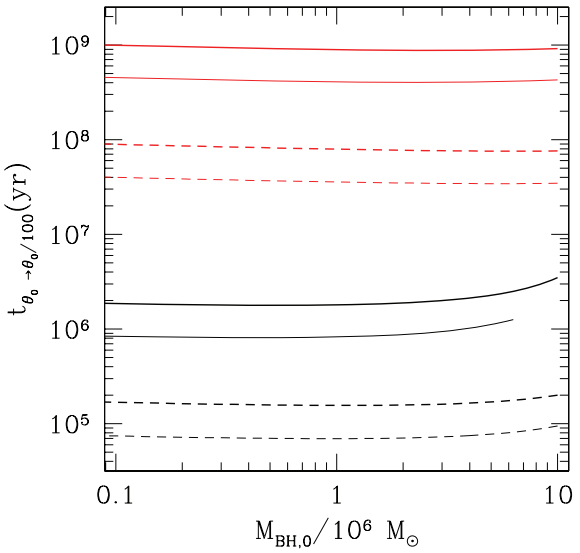

Figure 10. Alignment time (defined as the time needed for the relative inclination angle to reduce of two orders of magnitude, going from $\pi/6$ to $\pi/600$), as a function of the initial BH mass, $M_{\rm BH,0}$, for constant viscosity profile. The black lines refer to $f_{\rm Edd} = 1$ and the red ones to $f_{\rm Edd} = 0.001$; the solid lines are for initial spin parameter $a_0 = 0.9$ while the dashed ones $a_0 = 0.1$; finally, the thin lines represent $\alpha = 0.09$ and the thick ones $\alpha = 0.18$.

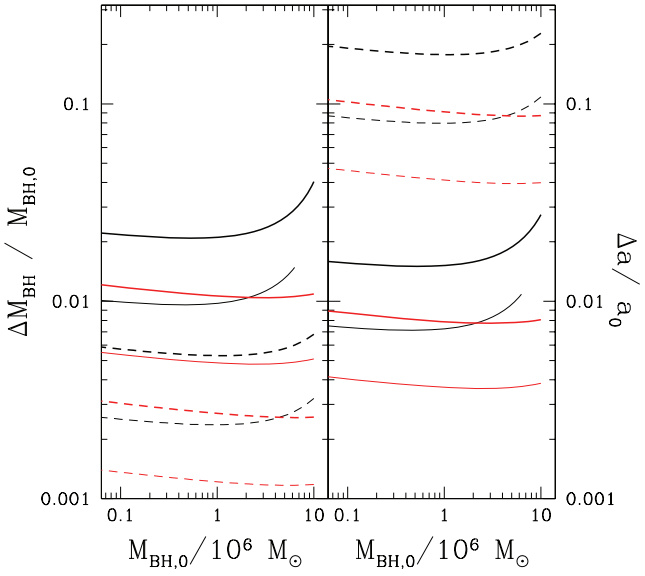

Figure 11. Mass and spin relative increase during the alignment time (defined as the time needed for the relative inclination angle to reduce of two orders of magnitude, going from $\pi/6$ to $\pi/600$) as a function of the initial BH mass, for constant viscosity profile. Black (red) lines refer to $f_{\rm Edd} = 1$ ($f_{\rm Edd} = 0.001$). Solid (dashed) lines are for $a_0 = 0.9$ ($a_0 = 0.1$); finally, the thin (thick) lines represent $\alpha = 0.09$ ($\alpha = 0.18$).

mass and spin parameter increases, for eight different sets of the other parameters. Comparing numerical scaling factors for M_6 in $\Delta t_{\theta_0 \to \theta_0/100}$ with that of expression (43), we note again a good agreement, in particular for $f_{\rm Edd}$ not too close to the Eddington limit and $M_{\rm BH,0} \lesssim 10^6\,{\rm M}_\odot$.

By contrast, the alignment process is more sensitive on $f_{\rm Edd}$, a_0 and α. Colour-coded maps of $\Delta t_{\theta_0 \to \theta_0/100}$ (Fig. 12), of $\Delta M/M_{\rm BH,0}$ (Fig. 13) and of $\Delta a/a_0$ (Fig. 14) are constructed in the a_0 versus

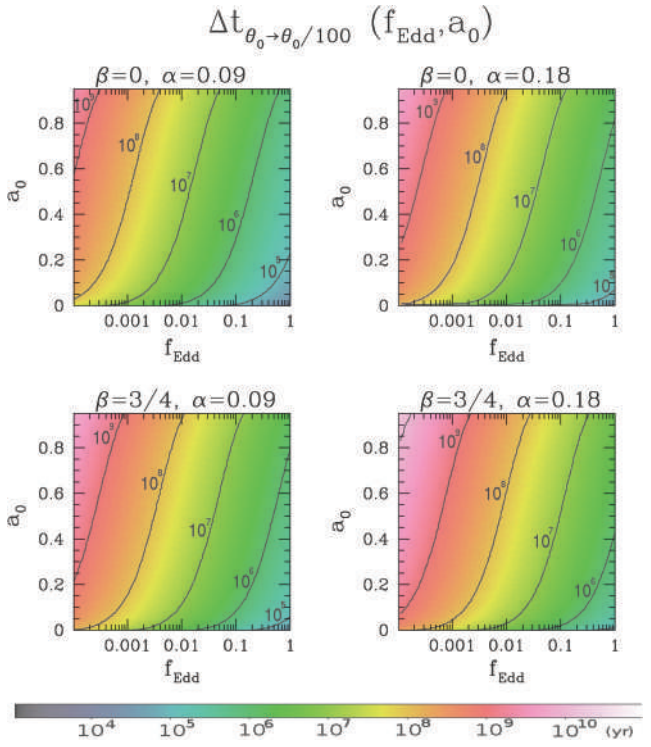

Figure 12. Colour-coded map of the alignment time (defined as the time necessary for the relative inclination angle to go from $\theta_{\rm out,0} = \pi/6$ to $\theta_{\rm out} = \pi/600$) for a BH of $M_{\rm BH,0} = 10^6\,{\rm M}_\odot$, as a function of the accretion rate expressed through the Eddington factor $f_{\rm Edd}$ and of the initial BH spin parameter a_0. The colour scale represents $t_{\rm al}$ in years. Top (bottom) panels refer to the constant (power-law) viscosity profile. Left-hand (right-hand) panels refer to $\alpha = 0.09$ ($\alpha = 0.18$).

$f_{\rm Edd}$ plane, varying the coefficient α and the viscosity law inside the accretion disc.

In Fig. 12, we infer the interval of the alignment time $\Delta t_{\theta_0 \to \theta_0/100}$ (as inferred from the numerical model) of interest for the study of BH evolution. The alignment time can vary by many orders of magnitude from $\sim 10^5$ to $\sim 10^{10}$ yr, and it reveals strong dependencies both on the accretion rate and on the initial spin parameter. In addition, smaller viscosities ($\alpha = 0.09$) give shorter time-scales compared to higher viscosities ($\alpha = 0.18$). A simple comparison between alignment times $\Delta t_{\theta_0 \to \theta_0/100}$ for different initial spin parameters, but identical $f_{\rm Edd}$, reveals that the scaling factors for a and $\eta_{0.1}(a)$ in equation (43) are in good agreement with numerical results.

Fig. 13 shows that the relative amount of mass accreted during the alignment process is small, compared to the initial BH mass. It varies between $\sim 10^{-3}$ and $\sim 10^{-2}$ for the constant viscosity profile, and between $\sim 2.5 \times 10^{-3}$ and $\sim 3 \times 10^{-2}$ for the power-law viscosity profile. Even if the accretion rate varies over four orders of magnitude, there are no comparable variations for the relative BH mass growth, in fact a larger $f_{\rm Edd}$ means a larger accretion rate, but it also reduces the alignment time. The relative increase of the spin parameter a is shown in Fig. 14. The evolution of a is the combination of different, and sometime opposite, tendencies: a highly spinning BH requires a longer time to align, but the particles at its innermost stable orbit carry on the BH a smaller angular momentum. The spin modulus increases significantly during the alignment for initially slowly rotating BHs and high accretion rates, typically with $5 \times 10^{-3} \lesssim \Delta a/a_0 \lesssim 8 \times 10^{-2}$ for a constant

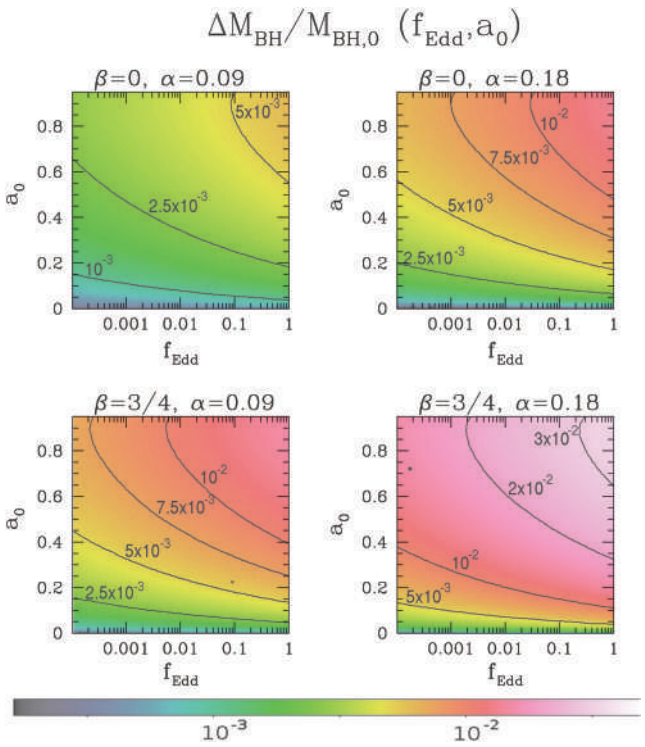

Figure 13. Colour-coded map of the relative increase of mass during the alignment time (defined as the time necessary for the relative inclination angle to go from $\theta_{\rm out,0} = \pi/6$ to $\theta_{\rm out} = \pi/600$) for a BH of $M_{\rm BH,0} = 10^6\,{\rm M}_\odot$, as a function of the accretion rate expressed through the Eddington factor $f_{\rm Edd}$ and of the initial BH spin parameter a_0. The colour scale represents $\Delta M_{\rm BH}/M_{\rm BH,0}$. Top (bottom) panels refer to the constant (power-law) viscosity profile. Left-hand (right-hand) panels refer to $\alpha = 0.09$ ($\alpha = 0.18$).

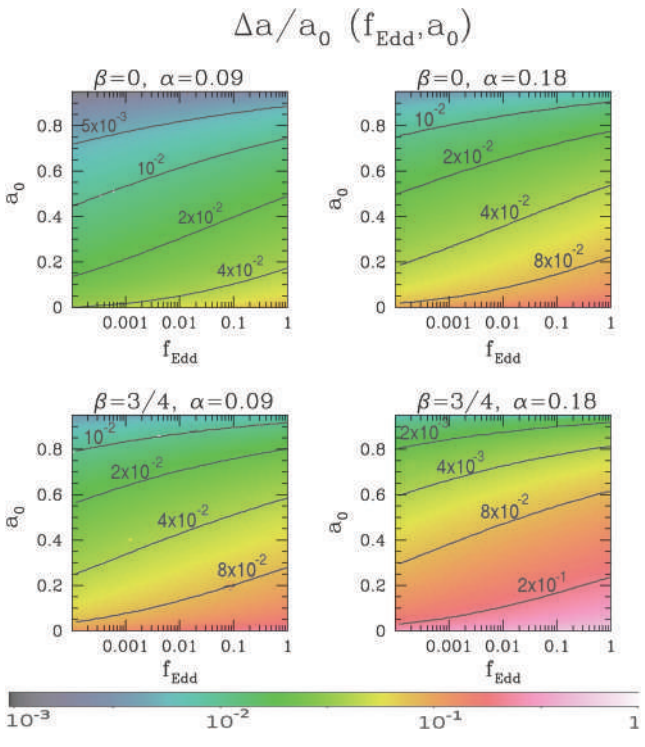

Figure 14. Colour-coded map of the relative increase of spin parameter during the alignment time (defined as the time necessary for the relative inclination angle to go from $\theta_{\rm out,0} = \pi/6$ to $\theta_{\rm out} = \pi/600$) for a BH of $M_{\rm BH,0} = 10^6\,{\rm M}_\odot$, as a function of the accretion rate expressed through the Eddington factor $f_{\rm Edd}$ and of the initial BH spin parameter a_0. The colour scale represents $\Delta a/a_0$. Top (bottom) panels refer to the constant (power-law) viscosity profile. Left-hand (right-hand) panels refer to $\alpha = 0.09$ ($\alpha = 0.18$).

viscosity profile and $10^{-2} \lesssim \Delta a/a_0 \lesssim 2 \times 10^{-1}$ for a power-law profile.

5.4 Counter-rotating case

In this section, we investigate the counter-rotating configuration for a BH and its misaligned accretion disc, for initial values of $\theta_{\rm out,0}$ close to π.

As shown by Scheuer & Feiler (1996) and Martin et al. (2007), on the time-scale $t_{\rm al}$ the BH spin again aligns with the outer regions of the accretion disc, if this disc is regularly and coherently fed. Due to the Bardeen–Petterson effect, we expect the innermost part of the disc (approximately within $R_{\rm warp}$) to orbit in a plane which is perpendicular to $\boldsymbol{J}_{\rm BH}$, with orbital angular momentum density $\boldsymbol{L}$ counteraligned with respect to the BH spin. In this BH–disc configuration, one of the major changes is in the radius of the innermost stable orbit, which increases due to the asymmetry seeded in the geodetic motion of particles in Kerr metrics. As a consequence, the energy and the orbital angular momentum of particles at $R_{\rm ISO}$ increase, while the BH radiative efficiency decreases (see e.g. Wilkins 1972; Bardeen et al. 1972). The Bardeen–Petterson time-scale (18) and the warp radius (19) have the same values as in the corotating case. Since $t_{\rm BP} \ll t_{\rm al}$, the adiabatic approximation holds again, but the small deformation approximation[2] has a limited validity, requiring $\theta_{\rm out} \sim \pi$. In order to remain consistent with the approximation scheme, we trace the alignment process, from π to $(\pi - \pi/6)$, only.

In the couter-rotating case and small deformation approximation (i.e. $\theta_{\rm out} \sim \pi$), the disc profile can be solved analytically. We choose a reference frame $O''x''y''z''$ where $\hat{\boldsymbol{J}}_{\rm BH} = (0, 0, -1)$ and we solved equation (14) for $\hat{\boldsymbol{l}}$ in it. For constant viscosities, the function $W''(R/R_{\rm warp}) = \hat{l}''_{\rm x} + i\hat{l}''_{\rm y}$ describing the warp is

$$W''_{\rm C,cnt} = C \exp\left[-\sqrt{2}(1+i)\left(\frac{R}{R_{\rm warp}}\right)^{-\frac{1}{2}}\right], \qquad (55)$$

while for a power-law viscosity profile

$$W''_{\rm PL,cnt} = D\left(\frac{R}{R_{\rm warp}}\right)^{-\frac{1}{4}} \times K_{1/2(1+\beta)}\left[\frac{\sqrt{2}(1+i)}{(1+\beta)}\left(\frac{R}{R_{\rm warp}}\right)^{-\frac{1+\beta}{2}}\right]. \qquad (56)$$

We then apply the adiabatic approximation to study the coupled evolutions of the system BH–disc. The jointed evolutions of $\theta_{\rm out}$, $M_{\rm BH}$ and a are presented in Fig. 15 and Table 3, for different accretion rates and viscosity profiles. The shorter time-scales in the counter-rotating configuration stem from the dependence of the alignment time-scale on the spin modulus, $t_{\rm al} \propto a^{5/7}$. Counter-rotating matter carries larger and opposite angular momentum, reducing the spin modulus and the alignment time-scale in the process.

[2] The functions ψ and χ, defined in equations (22) and (30), are invariant under the transformation $\theta_{\rm out} \to (\pi - \theta_{\rm out})$.

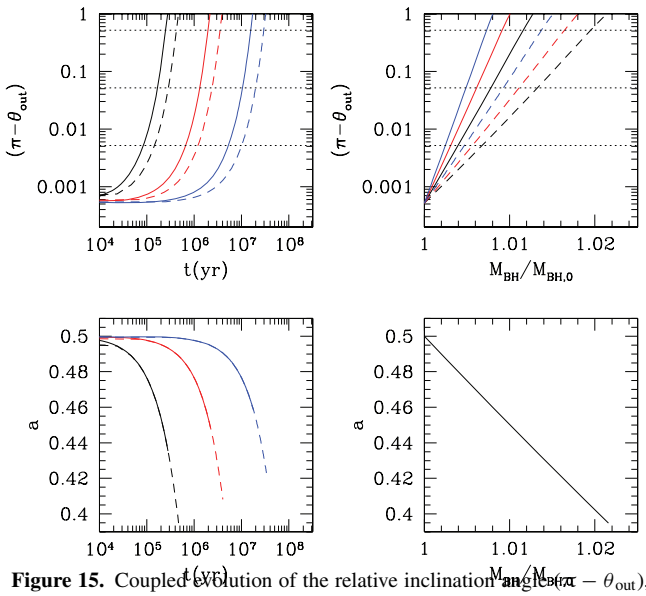

Figure 15. Coupled evolution of the relative inclination angle $(\pi - \theta_{\rm out})$, BH mass $M_{\rm BH}$ and spin parameter a for a counter-rotating disc. Solid (dashed) lines refer to constant (power-law) viscosity profile. Black lines to $f_{\rm Edd} = 1$, red lines to $f_{\rm Edd} = 0.1$, blue lines to $f_{\rm Edd} = 0.01$. Dotted horizontal lines which appear in top panels represent angles $\theta_{\rm out}/\theta_{\rm out,0} = 10, 10^2, 10^3$. Initial configuration: $M_{\rm BH,0} = 10^6\,{\rm M}_\odot$, $a_0 = 0.5$, $f_{\rm Edd} = 0.1$ and $\alpha = 0.09$, with $\pi - \theta_{\rm out,0} = \pi/600$.

6 DISCUSSION AND CONCLUSIONS

In this paper, we followed the joint evolution of the mass $M_{\rm BH}$ and spin $\boldsymbol{J}_{\rm BH}$ of a BH inside a geometrically thin, extended accretion disc. The BH spin is initially misaligned with the angular momentum of the disc in its outer regions. On the short Bardeen–Petterson time-scale, the disc responds to the Lense–Thirring precession, imposed by the BH spin, and propagates a warp that is maximum around $R_{\rm warp}$; within this radius, matter orbits around the BH in a plane which is perpendicular to the BH spin. According to angular momentum conservation, the warped disc interacts with the BH spin and, on the longer alignment time-scale the BH aligns its spin to $\hat{\boldsymbol{J}}_{\rm disc,out}$. In its outer regions, the disc is assumed to be fed by matter that flows along a plane that keeps its coherence in direction $\hat{\boldsymbol{J}}_{\rm disc,out}$ for a sufficiently long time-scale to allow for the gravitomagnetic interaction to complete BH–disc alignment. While doing so the BH is accreting matter and angular momentum from the inner portion of the disc, which is aligned or anti-aligned to the BH spin. Given the mismatch between the time-scale for warp propagation and the alignment time (Scheuer & Feiler 1996; Natarajan & Pringle 1998), we devised a method that enabled us to follow, in the small-deformation approximation, the co-evolution of the BH mass and spin in a self-consistent manner, carrying out a large survey of the parameter space and a critical review of the used approximations.

It is found that, considering an initial small relative inclination angle ($\theta_{\rm out,0} \lesssim \pi/6$, small deformation approximation), matter in the inner part of the accretion disc has orbital angular momentum density parallel to $\boldsymbol{J}_{\rm BH}$. The gravitomagnetic interaction of the BH with this warped accretion disc and their coupled evolution bring the BH into alignment with the outer regions of the disc, i.e. $\theta_{\rm out}(t) \to 0$. The time-scale $t_{\rm al}$ of equation (43) gives a good estimate of the BH–disc alignment time for an e-folding reduction of the angle of misalignment, in very good agreement with numerical results. For a maximally rotating Kerr BH accreting at the Eddington rate, $t_{\rm al} \sim 10^{5-6}$ yr, depending on the viscosity parameter α and on the

Table 3. Summary of our parameters and results for the counter-rotating case; we consider viscosity coefficient $\alpha = 0.09$ and initial inclination angle $\theta_{\rm out,0} = \pi(1 - 1/6000)$, both for constant (C) and power-law (PL) viscosity profiles (VP).

VP	$f_{\rm Edd}$	$(\pi - \theta_{\rm out})/(\pi - \theta_{\rm out,0})$	Δt (10^6 yr)	$\Delta M_{\rm BH}/M_{\rm BH,0}$ (in units of 10^{-2})	$\Delta a/a_0$ (in units of 10^{-2})
C	1	10	0.085	0.40	−3.99
		10^2	0.17	0.78	−7.81
		10^3	0.25	1.16	−11.5
	0.1	10	0.66	0.31	−3.12
		10^2	1.31	0.61	−6.15
		10^3	1.96	0.91	−9.11
	0.01	10	5.29	0.25	−2.49
		10^2	10.5	0.49	−4.92
		10^3	15.7	0.73	−7.31
PL	1	10	0.15	0.68	−6.79
		10^2	0.29	1.33	−13.1
		10^3	0.42	1.95	−19.1
	0.1	10	1.21	0.57	−5.68
		10^2	2.38	1.11	−11.0
		10^3	3.52	1.64	−16.2
	0.01	10	10.1	0.47	−4.73
		10^2	19.9	0.93	−9.24
		10^3	29.5	1.37	−13.6

Note. The initial BH has $M_{\rm BH,0} = 10^6\,{\rm M}_\odot$ and $a_0 = 0.5$. Accretion rate $f_{\rm Edd}$ varies over three orders of magnitude and we record times needed to $(\pi - \theta_{\rm out}, 0)$ of a factor 10, 100 or 1000; we also report mass and spin relative variations.

viscosity profile model, in agreement with early findings by Natarajan & Pringle (1998). On the other hand, environments where the accretion rate is extremely low imply longer alignment time-scales, as $t_{\rm al} \propto \dot{M}^{-32/35}$. In the explored BH mass range, the alignment time displays a weak dependence on $M_{\rm BH,0}$: fixed all the other parameters, alignment of a 10^7 $\rm M_\odot$ BH occurs, on average, at the same pace of a $10^5\,\rm M_\odot$ BH. The BH mass and spin modulus increase during alignment, but their fractional increases are modest. After surveying a wide parameter space, we find that $0.1 \lesssim \Delta M_{\rm BH}/M_{\rm BH,0} \lesssim 3$ per cent while the spin parameter increases by $0.5 \lesssim \Delta a/a_0 \lesssim 20$ per cent.

Starting with an almost antiparallel BH–disc configuration ($\theta_{\rm out,0} \approx \pi$), the orbital angular momentum density of the inner part of the disc is initially counter-aligned with respect to the BH spin. Nevertheless, the BH still tends to reduce the degree of misalignment [i.e. $\theta_{\rm out}(t)$ decreases], because of the nature of the gravitomagnetic interaction (see also Scheuer & Feiler 1996; Martin et al. 2007). The accretion of matter with opposite angular momentum at $R_{\rm ISO}$ decreases $\boldsymbol{J}_{\rm BH}$ and a with higher rates, compared with their growths in the specular corotating case. Since $t_{\rm al} \propto a^{5/7}$, the alignment process is then more efficient, i.e. the angle reduction speed is higher. Comparing decreases of the relative inclination angle $\theta_{\rm out}$ symmetric with respect to $\pi/2$, we find that the fractional decrease of the spin parameter in the counter-rotating case is, in modulus, higher than in the specular corotating case while the mass relative increase is slightly lower. BH spin flip, due to $\theta_{\rm out}$ reduction below $\pi/2$, will occur in this extended disc when a will reach its minimum value. At that time the jet of relativistic particles (if present) will cross the warped disc, likely affecting the subsequent BH–disc evolution and the BH feeding. This process deserves a separate investigation.

It is still poorly known whether a spinning BH in an active galactic nucleus (AGN) is fed through a disc that maintains its angular momentum direction *stable* over a Salpeter time-scale $t_{\rm S}$. Two opposite, still plausible scenarios, have been proposed and discussed. Natarajan & Pringle (1998) speculated that the stability of jets in radio-loud AGN requires a long-lived phase of stable accretion capable to maintain spatial coherence, i.e. a fixed direction of $\boldsymbol{J}_{\rm disc,out}$, for a time as long as 10^8 yr. By contrast, King & Pringle (2006, 2007) and King, Pringle & Hofmann (2008) speculated recently that AGN activity, triggered by gas-rich major mergers, is chaotic in nature even within a single merger event, i.e. occurring through a sequence of uncorrelated short-lived accretion episodes. In their picture, the corresponding discs, truncated by their own-self gravity, continuously change their inclination and feed the BH on their consumption time-scale. Under these circumstances, the BH spin modulus is seen to either increase or decrease at random clustering around small average values $a \sim 0.1$–0.3. This model would simultaneously explain the relatively low radiative efficiency of the quasar population as inferred from the background light (e.g. Merloni 2004; Merloni & Heinz 2008), and the possibility of growing BH as massive as $10^9\,\rm M_\odot$ from small BH seeds already at redshift $z \sim 6$ (King & Pringle 2006).

Isolated discs, truncated by their own self-gravity, carry a well-defined disc angular momentum and are accreted by the BH on a finite time-scale. Starting with a misaligned BH–disc configuration, the BH spin changes direction significantly only if (i) the alignment time is shorter than the disc consumption time, $t_{\rm al} < t_{\rm disc}$, and (ii) the magnitude of the disc angular momentum is comparable to the BH spin magnitude, i.e. $J_{\rm disc} \gtrsim J_{\rm BH}$. The first condition is verified for the whole parameter range explored in this paper. The estimate $J_{\rm disc} \gtrsim J_{\rm BH}$ depends instead sensitively upon $R_{\rm out}$. Equation (12) establishes that isolated discs around large BHs truncate at $R_{\rm out}$ such that $J_{\rm disc} < J_{\rm BH}$. Condition (ii) is satisfied for BH masses $\lesssim 3 \times 10^7\,\rm M_\odot$. We note here that since we model our discs using the Shakura–Sunyaev solution for Kramer's opacity, we cannot rigorously estimate $R_{\rm out}$, and $J_{\rm disc}$, for BHs with mass $\lesssim 10^5$–$10^6\,\rm M_\odot$. An extension of disc solutions to different, self-consistent opacities is non-trivial (Hure et al. 1994a,b) and we postpone a detailed analysis to future work.

BHs with masses $\lesssim 3 \times 10^7$ align efficiently in discs truncated by their own self-gravity, implying alignment also in the case of stochastically fed AGN,[3] where not only a fluctuates with time, but also the direction of the BH spin continually changes due to the rapidity of the alignment process. By contrast, rapidly spinning ($a \sim 1$) heavier BHs with $M_{\rm BH} \gtrsim 10^8\,\rm M_\odot$ have truncated discs that carry little angular momentum compared with $J_{\rm BH}$. In this case, alignment is uneffective and the orientation of the BH spin is not influenced significantly by the surrounding short-lived disc.

In light of these findings, the vector $\boldsymbol{J}_{\rm BH}$ appears to carry precious information on the orientation of the plane through which the BH has been fed, and on whether accretion has been long-lived and coherent or short-lived and random.

The method developed in the paper is sufficiently versatile that it will be implemented in numerical simulations describing the process of pairing of dual BHs in circumnuclear discs during their on-fly accretion (Dotti et al., in preparation) to improve upon the speculation (Bogdanović, Reynolds & Miller 2007) that, in gas-rich galaxy mergers, binary BHs have time to align their spin orthogonally to their orbital plane, as discussed in Escala et al. (2005), Dotti, Colpi & Haardt (2006), Mayer et al. (2007), Dotti et al. (2007, 2009) and Colpi & Dotti (2009). The spin–orbit configuration is relevant to study the impact of BH recoils, that occur after two BHs have coalesced (see e.g. Pretorius 2008). Detection of gravitational waves, emitted by coalescing BHs, with the *Laser Interferometer Space Antenna* (Bender et al. 1994; Hils & Bender 1995) will be able to constrain the moduli and the directions of the coalescing BHs spins (Vecchio 2004; Lang & Hughes 2006).

ACKNOWLEDGMENTS

We wish to thank Vittorio Gorini, Sergio Cacciatori, Alberto Sesana, Bernadetta Devecchi, Oliver Piattella and Luca Rizzi for usefull discussions and suggestions.

REFERENCES

Armitage P. J., Natarajan P., 1999, ApJ, 525, 909
Bardeen J. M., 1970, Nat, 226, 64
Bardeen J. M., Petterson J. A., 1975, ApJ, 195, L65
Bardeen J. M., Press W. H., Teukolsky S. A., 1972, ApJ, 178, 347
Bender P. et al., 1994, in Reinhard R., ed., LISA, Laser Interferometer Space Antenna for gravitational wave measurements: ESA Assessment Study Report. ESTEC, Noordwijk

[3] Here, we are not considering accretion events involving a disc with a very small amount of mass, i.e. below $\sim (H/R)M_{\rm BH}$. This light accretion disc has an outer radius much smaller than (9) and thus carries an angular momentum $J_{\rm disc} \ll J_{\rm BH}$. As a consequence, the disc has a very short consumption time-scale, and the alignment process is active for a very short period of time. Therefore the alignment of $\boldsymbol{J}_{\rm BH}$ around $\boldsymbol{J}_{\rm tot}$ (close to $\boldsymbol{J}_{\rm BH}$) is expected to be unimportant.

Bogdanović T., Reynolds C. S., Miller M. C., 2007, ApJ, 661, L147
Colpi M., Dotti M., 2009, Advanced Sci. Lett., preprint (arXiv:0906.4339)
Di Matteo T., Springel V., Hernquist L., 2005, Nat, 433, 604
Dotti M., Colpi M., Haardt F., 2006, MNRAS, 367, 103
Dotti M., Colpi M., Haardt F., Mayer L., 2007, MNRAS, 379, 956
Dotti M., Ruszkowski M., Paredi L., Colpi M., Volonteri M., Haardt F., 2009, MNRAS, 396, 1640
Escala A., Larson R. B., Coppi P. S., Mardones D., 2005, ApJ, 630, 152
Fragile P. C., Anninos P., 2005, ApJ, 623, 347
Fragile P. C., Blaes O. M., Anninos P., Salmonson J. D., 2007, ApJ, 668, 417
Frank J., King A., Raine D. J., 2002, Accretion Power in Astrophysics, 3rd edn. Cambridge Univ. Press, Cambridge, p. 398
Gammie C. F., Shapiro S. L., McKinney J. C., 2004, ApJ, 602, 312
Hils D., Bender P. L., 1995, ApJ, 445, L7
Hure J.-M., Collin-Souffrin S., Le Bourlot J., Pineau des Forets G., 1994a, A&A, 290, 19
Hure J.-M., Collin-Souffrin S., Le Bourlot J., Pineau des Forets G., 1994b, A&A, 290, 34
King A. R., Lubow S. H., Ogilvie G. I., Pringle J. E., 2005, MNRAS, 363, 49
King A. R., Pringle J. E., 2006, MNRAS, 373, L90
King A. R., Pringle J. E., 2007, MNRAS, 377, L25
King A. R., Pringle J. E., Livio M., 2007, MNRAS, 376, 1740
King A. R., Pringle J. E., Hofmann J. A., 2008, MNRAS, 385, 1621
Lang R. N., Hughes S. A., 2006, Phys. Rev. D, 74, 122001
Levin Y., 2007, MNRAS, 374, 515
Levine R., Gnedin N. Y., Hamilton A. J. S., Kravtsov A. V., 2008, ApJ, 678, 154
Lodato G., 2007, Nuovo Cimento Rivista Serie, 30, 293
Lodato G., Pringle J. E., 2006, MNRAS, 368, 1196
Lodato G., Pringle J. E., 2007, MNRAS, 381, 1287
Martin R. G., Pringle J. E., Tout C. A., 2007, MNRAS, 381, 1617
Mayer L., Kazantzidis S., Madau P., Colpi M., Quinn T., Wadsley J., 2007, Sci, 316, 1874
Merloni A., 2004, MNRAS, 353, 1035
Merloni A., Heinz S., 2008, MNRAS, 388, 1011
Mihos J. C., Hernquist L., 1996, ApJ, 464, 641
Natarajan P., Armitage P. J., 1999, MNRAS, 309, 961
Natarajan P., Pringle J. E., 1998, ApJ, 506, L97
Nelson R. P., Papaloizou J. C. B., 2000, MNRAS, 315, 570
Papaloizou J. C. B., Pringle J. E., 1983, MNRAS, 202, 1181
Polyachenko V. L., Polyachenko E. V., Strel'Nikov A. V., 1997, Astron. Lett., 23, 483
Pretorius F., 2008, APS Meeting Abstract, p. 6002
Pringle J. E., 1981, ARA&A, 19, 137
Pringle J. E., 1992, MNRAS, 258, 811
Rees M. J., 1978, Nat, 275, 516
Scheuer P. A. G., Feiler R., 1996, MNRAS, 282, 291
Shakura N. I., Syunyaev R. A., 1973, A&A, 24, 337
Thorne K. S., Price R. H., MacDonald D. A., 1986, Black Holes: The Membrane Paradigm. Yale Univ. Press, New Haven
Vecchio A., 2004, Phys. Rev. D, 70, 042001
Weinberg S., 1972, Gravitation and Cosmology: Principles and Applications of the General Theory of Relativity. Wiley, New York, p. 688
White S. D. M., Rees M. J., 1978, MNRAS, 183, 341
Wilkins D. C., 1972, Phys. Rev. D, 5, 814

APPENDIX A: EXPLICIT EXPRESSIONS OF THE GRAVITOMAGNETIC TORQUE

Constant viscosity: for the constant viscosity model, the disc profile is described by (29) and the equation (53) becomes

$$\delta(J_{\mathrm{BH},x}+iJ_{\mathrm{BH},y})_{\mathrm{gm}} = (1-i)\frac{2\sqrt{2}A}{3}\sqrt{GM_{\mathrm{BH}}}\frac{G\dot{M}J_{\mathrm{BH}}}{A_{\nu_1}c^2R_{\mathrm{warp}}^{5/4}}t_{\mathrm{BP}}(R_{\mathrm{warp}}) \times \exp\left[-\sqrt{2}(1-i)\left(\frac{R}{R_{\mathrm{warp}}}\right)^{-1/2}\right]\Bigg|_{R_{\mathrm{ISO}}}^{R_{\mathrm{out}}}. \quad \text{(A1)}$$

Power-law viscosity: for the power-law case (4) with exponent β, the disc profile is given by W_{PL}, defined as (28). In this case, equation (53) was integrated by Martin et al. (2007):

$$\delta(J_{\mathrm{BH},x}+iJ_{\mathrm{BH},y})_{\mathrm{gm}} = -i\frac{8G\dot{M}J_{\mathrm{BH}}\sqrt{GM_{\mathrm{BH}}}}{3(1+\beta)A_{\nu_1}c^2} \times B\left(\frac{\sqrt{2}}{1+\beta}(1-i)\right)^{-\frac{4\beta+3}{2(1+\beta)}}R_{\mathrm{warp}}^{-\left(\beta+\frac{1}{2}\right)} \times t_{\mathrm{BP}}(R_{\mathrm{warp}})\int_{z_{\mathrm{in}}}^{z_{\mathrm{out}}} z^{\frac{2\beta+1}{2(1+\beta)}}K_{\frac{1}{2(1+\beta)}}(z)\,\mathrm{d}z, \quad \text{(A2)}$$

where z is a new complex variable, defined as

$$z = \frac{\sqrt{2}}{1+\beta}(1-i)\left(\frac{R}{R_{\mathrm{warp}}}\right)^{-\frac{1+\beta}{2}}. \quad \text{(A3)}$$

Assuming that

$$\int_{z_{\mathrm{in}}}^{z_{\mathrm{out}}} z^{\frac{2\beta+1}{2(1+\beta)}}K_{\frac{1}{2(1+\beta)}}(z)\,\mathrm{d}z \approx \int_0^{(1-i)\infty} z^{\frac{2\beta+1}{2(1+\beta)}}K_{\frac{1}{2(1+\beta)}}(z)\,\mathrm{d}z = 2^{-\frac{1}{2(1+\beta)}}\Gamma\left[\frac{1+2\beta}{2(1+\beta)}\right], \quad \text{(A4)}$$

we can rewrite the infinitesimal gravitomagnetic spin variation as

$$\frac{\delta(J_{\mathrm{BH},x}+iJ_{\mathrm{BH},y})_{\mathrm{gm}}}{J_BH} = i^{-\frac{1}{4(1+\beta)}}\frac{t_{\mathrm{BP}}(R_{\mathrm{warp}})}{T_{\mathrm{PL}}}, \quad \text{(A5)}$$

where

$$T_{\mathrm{PL}}^{-1} = \frac{4G\dot{M}\sqrt{GM_{\mathrm{BH}}}}{3A_{\nu_1}c^2}B\left(\frac{\sqrt{2}}{1+\beta}\right)^{-\frac{2\beta+1}{2(1+\beta)}} \times R_{\mathrm{warp}}^{-\left(\beta+\frac{1}{2}\right)}2^{-\frac{2\beta+3}{4(1+\beta)}}\Gamma\left[\frac{1+2\beta}{2(1+\beta)}\right]. \quad \text{(A6)}$$

Martin et al. (2007) estimate the alignment time-scale as

$$t_{\mathrm{al},M} = \frac{T_{\mathrm{PL}}}{\cos\left[\frac{\pi}{4(1+\beta)}\right]}. \quad \text{(A7)}$$

This paper has been typeset from a TEX/LATEX file prepared by the author.